Supporting Information of Programmed Supramolecular Assemblies using Orthogonal Pairs of Heterodimeric Coiled Coil Peptides

Linhai Jiang[a], Xiaobing Zuo[b], Jianping Li,[a] Nathaniel J. Traaseth[a] and Kent Kirshenbaum[a,*]

a: Chemistry Department, New York University, 100 Washington Square E, New York, NY, 10003, USA. E-mail: kk54@nyu.edu

b: X-ray Science Division, Argonne National Laboratory, Lemont, IL 60439, USA.

Materials

Dichloromethane (DCM), acetonitrile (ACN) and HPLC grade water were supplied by Pharmco. Tetrakis(triphenylphosphine)palladium(0) ($Pd(PPh_3)_4$), phenylsilane and N^{α}-Fmoc-N^{β}-allyloxycarbonyl-L-2,3-diaminopropionic acid (Fmoc-Dap(Alloc)-OH) were purchased form Chem Impex. All Fmoc-protected natural amino acids, rink amide MBHA resin, urea, acetic anhydride, *N, N*-diisopropylethylamine (DIEA), trifluoroacetic acid (TFA), formic acid, triisopropylsilane (TIPS), piperidine, *N, N*-dimethylformamide (DMF), 2-(6-Chloro-1-H-benzotriazole-1-yl)-1,1,3,3-tetramethylaminium hexafluorophosphate (HCTU), 1-[Bis(dimethylamino)methylene]-1H-1,2,3-triazolo[4,5-b]pyridinium 3-oxid hexafluorophosphate (HATU), cupric sulfate, potassium phosphate monobasic dihydrate, potassium phosphate dibasic dihydrate, aminoguanidine hydrochloride, potassium chloride and ethylenediaminetetraacetic acid (EDTA) were purchased from Milipore Sigma. Propargyl amine and 2-azido acetic acid were purchased from Tokyo Chemical Industry. L-ascorbic acid sodium salt was purchased from Acros Organics. Tris(benzyltriazolylmethyl)amine (THPTA) was purchased from Click Chemistry Tools. Deionized water was produced on site with an Elga water purification system.

Methods

Synthesis of Single Chain Peptides

General Method

An automated peptide synthesizer (Model: Prelude, Gyros Protein Technologies) was used to synthesize all the linear peptides through Fmoc-chemistry based solid phase peptide synthesis method. Typically, synthesis was carried out at 0.05 mmol scale by using rink amide MBHA resin as the solid support. The Fmoc groups were deprotected by mixing the resin with 5 ml cleavage solution containing formic acid, piperidine and DMF with a volume ratio of 1:20:79 for 5 minutes.[1] This step was repeated one more time for ensuring the complete removal of Fmoc groups. For the coupling of amino acids, 3 mL DMF solution containing 5 equivalents of Fmoc amino acid, 4.9 equivalents of HCTU and 10 equivalents of DIEA were added to the resins, and the reaction mixture was stirred for 1 hour. The deprotection-coupling cycle was iterated until the target amino acid sequence was achieved. Afterwards, 3 mL DMF solution containing 50 equivalents of acetic anhydride and 6 equivalents of DIEA was mixed with resin for 1 hour to cap the N-termini. The peptide was cleaved from resin by using a cleavage cocktail containing 2.5 vol% water, 2.5 vol% TIPS and 95 vol% TFA. The side chain protecting groups were removed simultaneously during the cleavage reaction (3-hr shaking). The cleaved product was washed three times with chilled diethyl ether. Reversed phase HPLC was conducted using a C18 column to purify the crude product using water and acetonitrile as the mobile phase. Collected HPLC fractions were then lyophilized for three days to obtain the purified peptide powders. The molecular weight of the desired product was confirmed using an Agilent 6120 single quadrupole LC-MS spectrometer and the purity was evaluated by analytical HPLC conducted using an Eclipse Plus C18 column.

*Modification of **4A** Peptide*

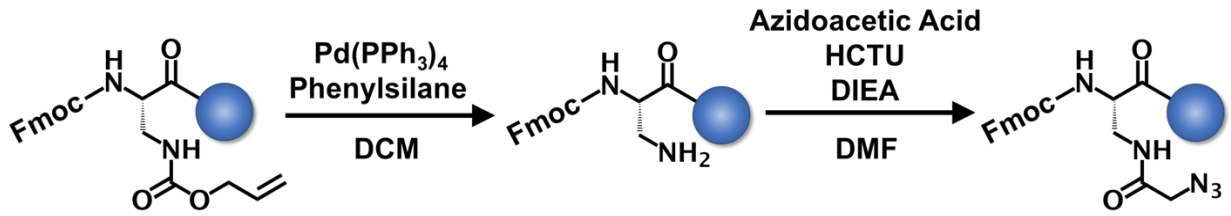

Scheme S1. Synthetic route for installing azido group at the C-terminus of **4A** peptide. The blue sphere repsents the resin.

The installation of azido group at the C-terminus of **4A** peptide is illustrated in Scheme S1. After the coupling of the first residue, Fmoc-Dap(Alloc)-OH, to the resin, the side chain protecting group was removed manually as follows: 1) the resin was washed with dry DCM three times, 2) the resin was then agitated 20 minutes with 3 mL dry DCM solution containing 0.25 equivalents of $Pd(PPh_3)_4$ and 24 equivalents of phenylsilane (note: the color of the reaction mixture changed from bright yellow to dark brown), 3) the DCM solution was removed and the resin was washed with dry DCM for three times, 4) step 2) and step 3) was repeated for two more times, and the resin was then washed thoroughly with DMF.

A 3 mL volume of DMF solution containing 5 equivalents of 2-azido acetic acid, 4.9 equivalents of HCTU and 10 equivalents of DIEA was then mixed with the resin for 1 hour. This step was repeated one more time to ensure the completion of the reaction. The peptide chain elongation was then continued on the automated peptide synthesizer.

N-terminal Capping for 4B Peptide

The N-terminus of **4B** peptide was capped differently than the other peptides. After the elongation of the desired peptide chain, 3 mL DMF solution containing 5 equivalents of 2-azido acetic acid, 4.9 equivalents of HCTU and 10 equivalents of DIEA was mixed with the resin for 1hour to install azido group at the N-terminus of **4B** peptide.

*Side Chain Modification of **5A1** and **5A2** Peptides*

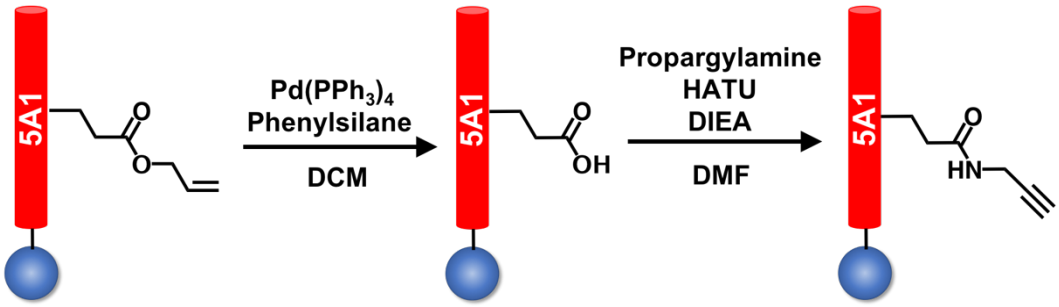

Scheme S2. Synthetic route of installing alkyne group in the side chain of **5A1** peptide. The blue sphere repsents the resin.

The side chain modification of **5A1** and **5A2** peptides were carried out after the acetylation of N-termini. The overall procedure is shown in **Scheme S2**, as exemplified for **5A1**. Briefly, the OAll protecting group of the Glu(OAll) monomer at residue 22 in **5A1** was removed in the same

way as the Alloc group was removed in the **4A** peptide. Afterwards, 1 mL DMF solution containing 10 equivalents of DIEA, 1 mL DMF solution containing 5 equivalents of HATU and 1mL DMF solution containing 15 equivalents of propargylamine were added to resin sequentially. The mixture was stirred for 1 hour. This coupling step was also repeated a second time to ensure the completion of the reaction.

The side chain modification of Glu(OAll) at residue 8 and Glu(OAll) at residue 36 in **5A2** were carried out in the same way as for **5A1**. The quantities of each chemical reagent were doubled but the reaction time was unchanged.

Conjugation by "CuAAC" Click Chemistry

The conjugation reactions were carried out by following a procedure we reported previously.[2] For a typical reaction to synthesize **Con_5A2-(4B)$_2$**, seven solutions were prepared separately as follows:

Solution A: 2.4 mg of **5A2** peptide (MW: 5508 Daltons) was dissolved in 1 mL potassium phosphate buffer (100 mM, pH=7.5).

Solution B: 5.1 mg of **4B** peptide (MW: 4827 Daltons) was dissolved in 15 mL potassium phosphate buffer (100 mM, pH=7.5). The mole ratio of azido groups in **4B** was 20% in excess relative to the alkyne groups in **5A2**.

Solution C: 2 M urea solution in deionized water.

Solution D: 20 mM copper (II) sulfate solution in deionized water.

Solution E: 100 mM THPTA solution in deionized water.

Solution F: 1 M aminoguanidine hydrochloride solution in deionized water.

Solution G: 1 M sodium ascorbate solution in deionized water.

A 0.534 mL aliquot of **solution D** was pre-mixed with 0.534 mL of **solution E**, and the mixture was then placed aside. To 20 mL scintillation vial, 1 mL of **solution A**, 15 mL of **solution B** and 0.534 mL of **solution C** were sequentially added. Afterwards, the pre-mixed mixture of **solution D** and **solution E** were added, followed by the addition of 0.534 mL of **solution F** and 0.534 mL of **solution G**. The scintillation vial was then capped. After being stirred for 24 hours, the colorless reaction mixture became dark yellow. Then, 5.4 mL of 20 mM EDTA/potassium phosphate buffer solution (100 mM, pH=7.5) was added to the reaction mixture and the mixture was filtered through PVDF filers with 200 nm pore size. Reversed phase HPLC was used to

separate the desired product from other species using water and acetonitrile as the mobile phase. Collected HPLC fractions were then lyophilized for three days. The molecular weight of the desired product was confirmed by using an Agilent 6120 single quadrupole LC-MS spectrometer and the purities were evaluated by analytical HPLC equipped with an Eclipse Plus C18 column.

Size Exclusion Chromatography Purification

The stock solutions of single-chain peptides and conjugated peptide were prepared by dissolving the lyophilized powders in a neutral (pH=7.5) buffer containing 12.5 mM potassium phosphate and 150 mM potassium chloride. The concentration was estimated from the UV absorbance at 280 nm of tyrosine or tryptophan using the respective molar absorptivities of 1490 $cm^{-1}M^{-1}$ and 5500 $cm^{-1}M^{-1}$. (Note: this concentration determination method is quite accurate for all single-chain peptides, but not for the conjugated peptide. The baseline of UV spectra measured for all single-chain peptides are sufficiently flat for accurate concentration estimation. However, the UV spectra of conjugated peptides are strongly associated with baseline drift, diminishing the accuracy of concentration determination)

To ensure that the desired stoichiometries are achieved for the heterodimeric coiled coils and other co-assemblies, size exclusion chromatography based purifications were carried out on ÄKTA Pure protein purification system equipped with a Superdex 75 10/300 GL column. All the samples were freshly prepared prior to SEC purification. A neutral (pH=7.5) buffer containing 12.5 mM potassium phosphate and 150 mM potassium chloride was used as the mobile phase. Amicon ultracentrifugation filters were used to concentrate the collected SEC fractions to desired concentrations for different biophysical characterizations.

Circular Dichroism Spectroscopy

The samples of individual single-chain peptides, conjugated peptides and mixtures of non-complementary pairs were prepared by directly dissolving the lyophilized powders in a neutral (pH=7.5) buffer containing 12.5 mM potassium phosphate and 150 mM potassium chloride. For mixture of complementary pairs, pre-barbell_A & B, barbell, pre-quadrilateral_A & B and quadrilateral shaped assemblies, the SEC purified fractions were used for CD measurements. The concentration of each sample was estimated from the UV absorbance at 280 nm of tyrosine or tryptophan using the molar absorptivities of 1490 $cm^{-1}M^{-1}$ and 5500 $cm^{-1}M^{-1}$, respectively.

The total peptide chain concentration of each sample was adjusted to be 0.01mM for all measurements. A Jasco J-1500 circular dichroism spectrometer was used for all CD studies. The heating rate for thermal denaturation experiments was set as 1 ºC/minute.

Size Exclusion Chromatography in-line with Multiangle Laser Scattering (SEC-MALS)

For each sample, the SEC purified fractions were used for SEC-MALS analysis. The concentration of each sample was adjusted to be in the range of 0.2-0.5 mg/mL. A SEC-MALS system equipped with Wyatt Dawn multi-angle light scattering detector, Wyatt Optilab T-rEX refractive index detector, Agilent 1260 HPLC system and Superdex 200 column was used for the measurements.

Small Angle X-ray Scattering (SAXS) Measurements

For samples used in SAXS measurements, 1 vol% of glycerol was added to the running buffer for SEC purifications. Afterwards, the collected fractions were concentrated by Amicon ultracentrifugation filters and the final concentrations were estimated by the UV absorbance at 280 nm of tyrosine or tryptophan using the molar absorptivities of 1490 $cm^{-1}M^{-1}$ and 5500 $cm^{-1}M^{-1}$, respectively.

SAXS experiments were performed at beamline 12-ID-B of the Advanced Photon Source, Argonne National Laboratory. Scattering data were obtained using an x-ray radiation of 14.0 keV and a detector distance of 2.0 m covering a Q-range of ~ 0.004 - 0.9 $Å^{-1}$ ($Q=4\pi\sin(\theta/2)/\lambda$, with λ the x-ray wavelength, and θ the scattering angle). The 2-D SAXS data reduction was performed using the beamline matlab software package, and the further SAXS data analyses were conducted using the BioXTAS package.[3]

Transmission Electron Microscopy

The SEC-purified quadrilateral-shaped assembly was used for TEM imaging. The concentration was adjusted to ~0.045 mg/mL. The sample was stained by uranyl acetate and imaged by FEI Talos L120C TEM with Gatan 4k x 4k OneView camera.

Molecular Dynamics Simulations

Constructions of initial computer models were performed in PyMOL by using in-house python scripts. First, the X-ray crystal structures of the parent coiled coil dimers of **4A/4B** (pdb id: 3HE4) and **5A/5B** dimer (pdb id: 3HE5) were adopted to generate the computer models of **4A/4B** dimer, **5A1/5B** dimer and **5A2/5B** dimer.[4] Before the construction of barbell and quadrilateral shaped assemblies, 1,4-triazole bonds were constructed between the acetylated propargylamine and the terminal azido group of **4A** and **4B** peptides (**Scheme S3**). The side chain carboxylic acid groups of Glu22 in **5A1**, Glu8 and Glu36 in **5A2** peptides were all capped by N-methyl amide groups (**Scheme S4**). Construction of the barbell shaped assemblies was carried out by following the flowchart shown in **Chart S1** and the quadrilateral shaped assemblies were constructed following the flowchart shown in **Chart S2**.

Molecular dynamics simulations were carried out using the Amber 20.11 package.[5] The ff19SB force field was used for modelling the natural amino acid components.[6] The amino acids containing triazole bonds in the side chains were modelled by using Amber-compatible TZLff parameters.[7] Explicit solvent, using the OPC water model,[8] was included for all MD simulations. The buffer distance between the peptide assemblies and simulation box boundary was set as 12 Å. Potassium ions were used to neutralize the overall negative charges of the barbell and quadrilateral shaped assemblies. A suitable number (depending on the volume of the equilibrated simulation box) of additional potassium ions and chloride ions were added to mimic the experimental ionic strength of 150mM. The SHAKE algorithm was used to constrain bonds involving hydrogen atoms. Force evaluation was set with a 10 Å cutoff for both Lennard-Jones interactions and electrostatic interactions calculated by smooth PME approach. The simulation temperature was controlled with a Langevin thermostat with a collision frequency of 1 ps^{-1}. For NPT runs, constant pressure (1bar) was controlled by a Monte Carlo barostat.

The MD equilibration was performed in nine steps by using the pmemd.MPI module and following the protocol reported by the Simmerling Lab.[6]

Step-1: Initial energy minimizations were performed by 10 steps of steep-descent method and 9990 steps of conjugate gradient method with a restraint of 100 kcal/mol/rad^2 applied to the heavy atoms in all residues except those including triazole groups in the side chains.

Step-2: The system was heated from 100K to 298K over 1 ns in NVT ensemble with the same restraint applied as in Step-1 and a time step of 1 fs.

Step-3: A 1-ns NPT run was performed in NPT ensemble with the same restraint applied as in Step-1 and pressure relaxation time of 0.1 ps.

Step-4: Another 1-ns NPT run was carried out with the pressure relaxation time increased to 0.5 ps and the restraint decreased to 10 kcal/mol/rad^2.

Step-5: The system was minimized again by 10 steps of steep-descent method and 9990 steps of conjugate gradient method with 10 kcal/mol/rad^2 restraint applied to the backbone C and N atoms.

Step-6: A 1-ns NPT run was performed with the same restraint applied as in step-5.

Step-7: The restraint was reduced to 1.0 kcal/mol/rad^2 for another 1-ns NPT run.

Step-8: The restraint was reduced to 0.1 kcal/mol/rad^2 for another 1-ns NPT run.

Step-p: A 1-ns NPT run was performed without any restraint.

The MD production runs were carried out by using pmemd.cuda module with a typical time scale of 500 ns. Three different runs were separately performed. Cpptraj package was used for converting the Amber mdcrd trajectory files to pdb format. FoXS package[9-10] was used to predict the theoretical SAXS profiles of each trajectory frame and evaluate the agreement to the experimental data. The frames that generated SAXS profiles with the best correspondence to the experimental data were used for statistical analysis.

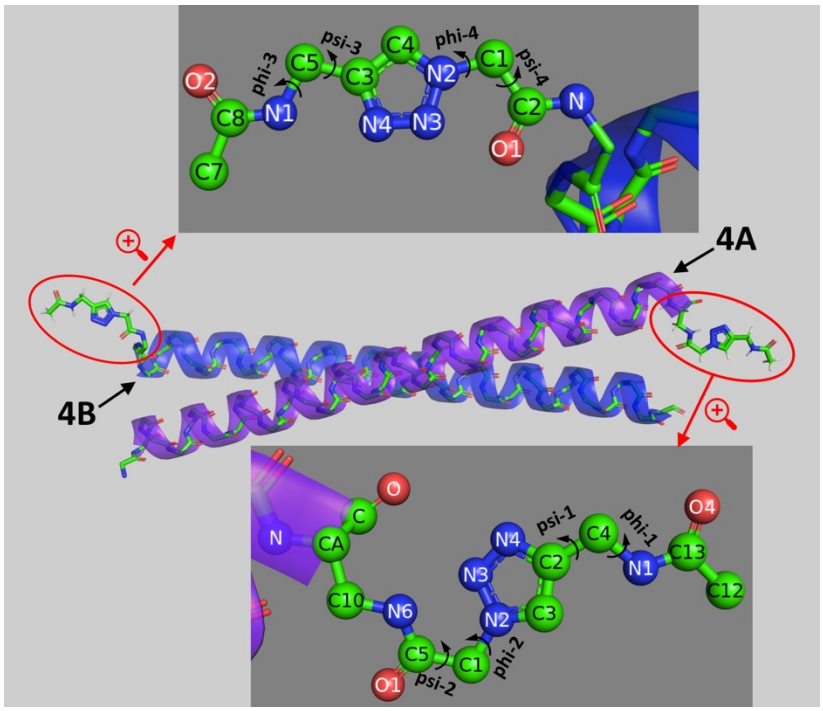

Scheme S3. Modifications made at the C- and N- termini of **4A/4B** dimer prior to the construction of the barbell and quadrilateral shaped assemblies.

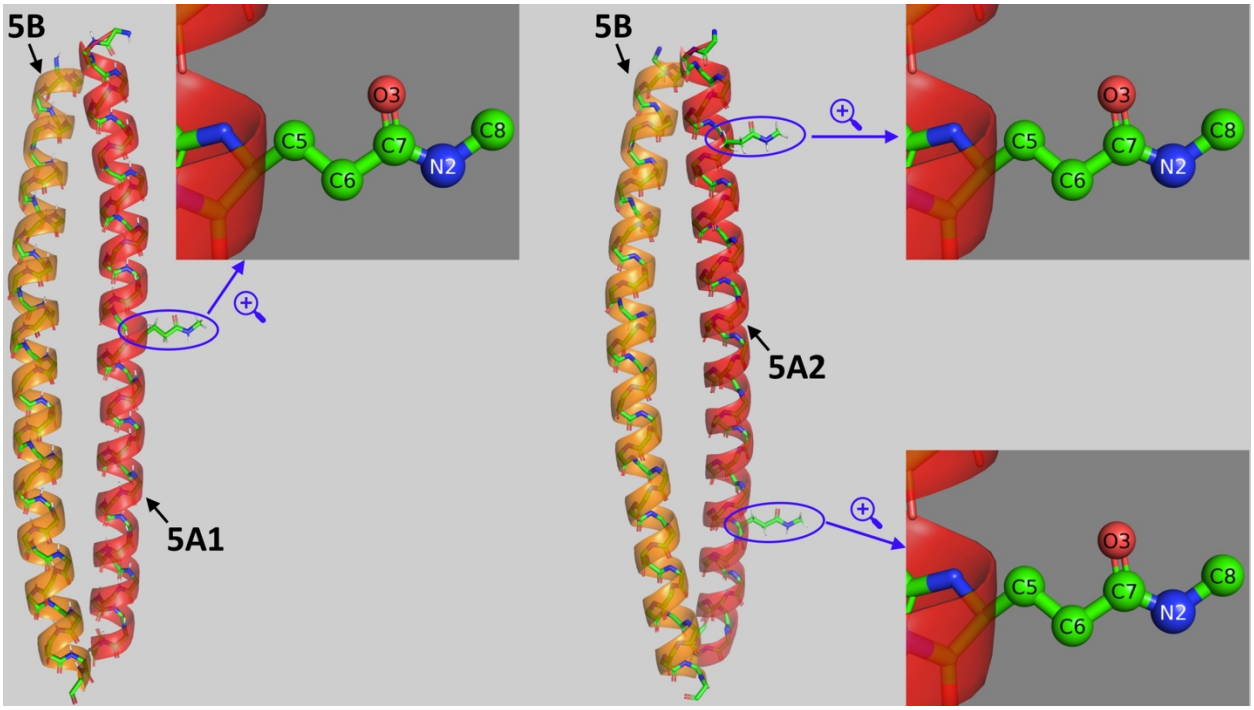

Scheme S4. Modifications made to the side chains of Glu at residue 22 in **5A1**, Glu at reisdue 8 and 36 in **5A2** prior to the construction of the barbell and quadrilateral shaped assemblies.

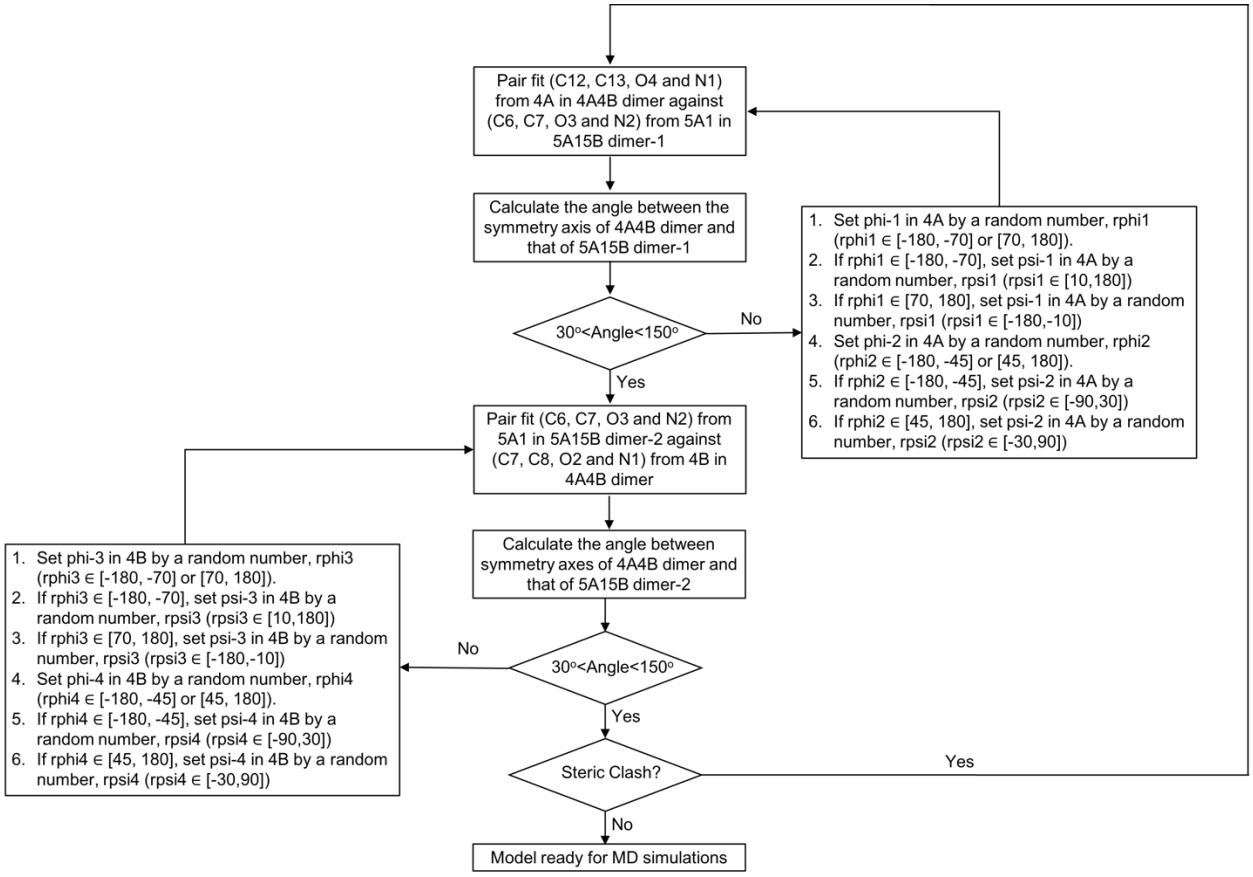

Chart S1. Flowchart for constructing the barbell shaped assemblies in silico. The allowed values of phi-1, psi-1, phi-2, psi-2, phi-3, psi-3, phi-4 and psi-4 dihedral angles are chosen based on the energy landscape reported in the literature.[7]

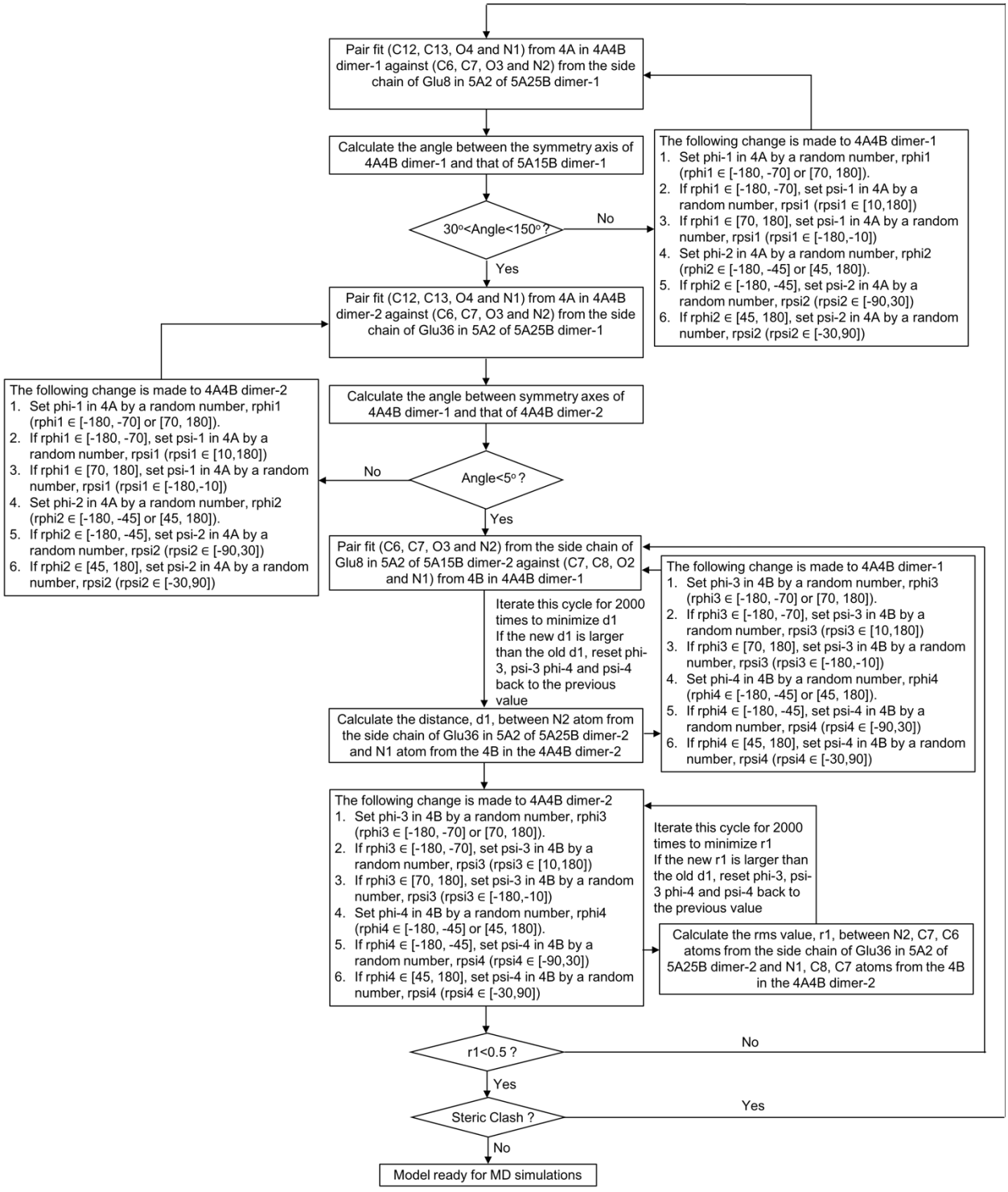

Chart S2. Flowchart for constructing the quadrilateral shaped assemblies in silico. The allowed values of phi-1, psi-1, phi-2, psi-2, phi-3, psi-3, phi-4 and psi-4 dihedral angles are chosen based on the energy landscape reported in the literature.[7]

Supplementary Data

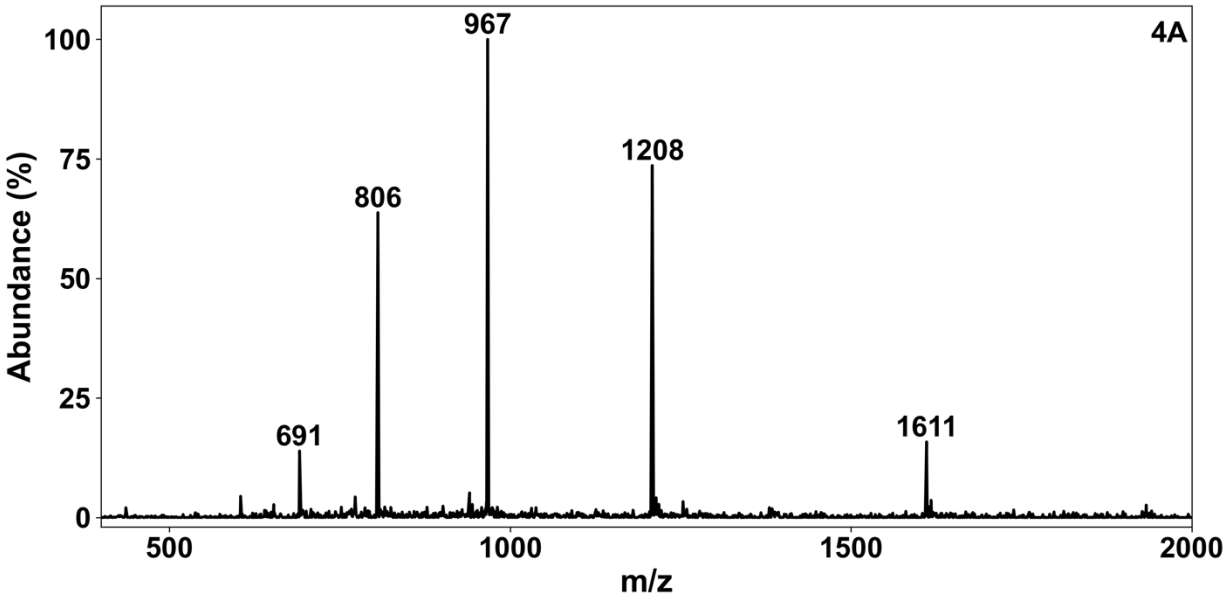

Figure S1. Mass spectrometry data of the **4A** peptide. Expected mass: $[M+H]^{+}/1=4832$, $[M+3H]^{3+}/3=1611$, $[M+4H]^{4+}/4=1209$, $[M+5H]^{5+}/5=967$, $[M+6H]^{6+}/6=806$, $[M+7H]^{7+}/7=691$.

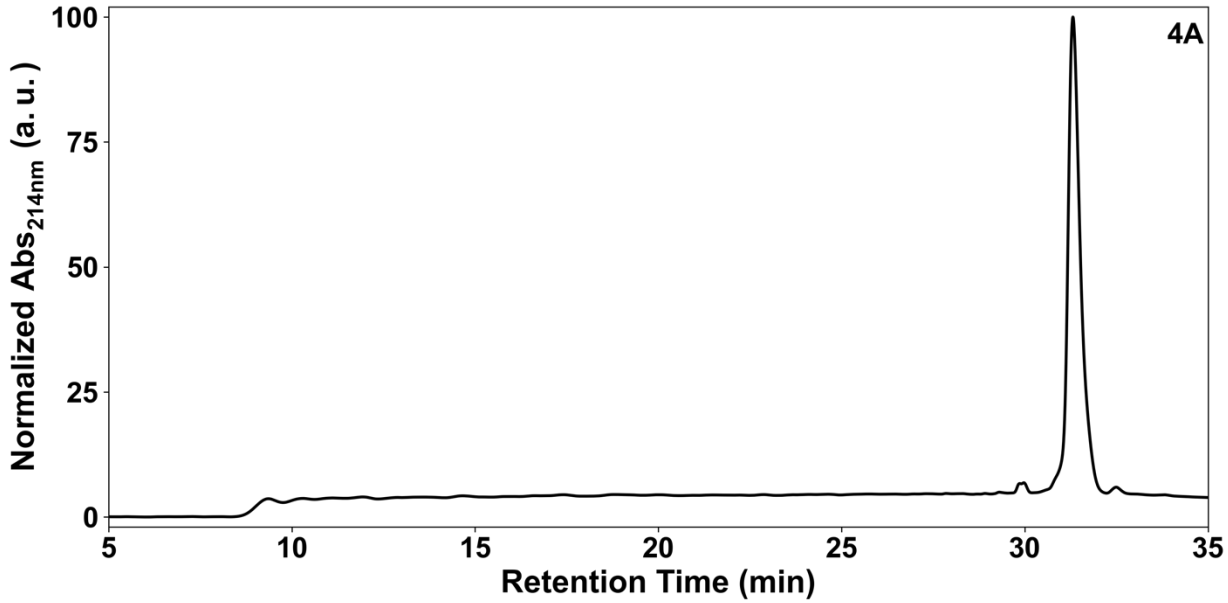

Figure S2. Analytical HPLC trace of the **4A** peptide. A linear gradient of ACN (0.1 vol% TFA) into H_2O (0.1 vol% TFA) over 30 min (5% ACN at 5 min, 95% ACN at 35min) was used.

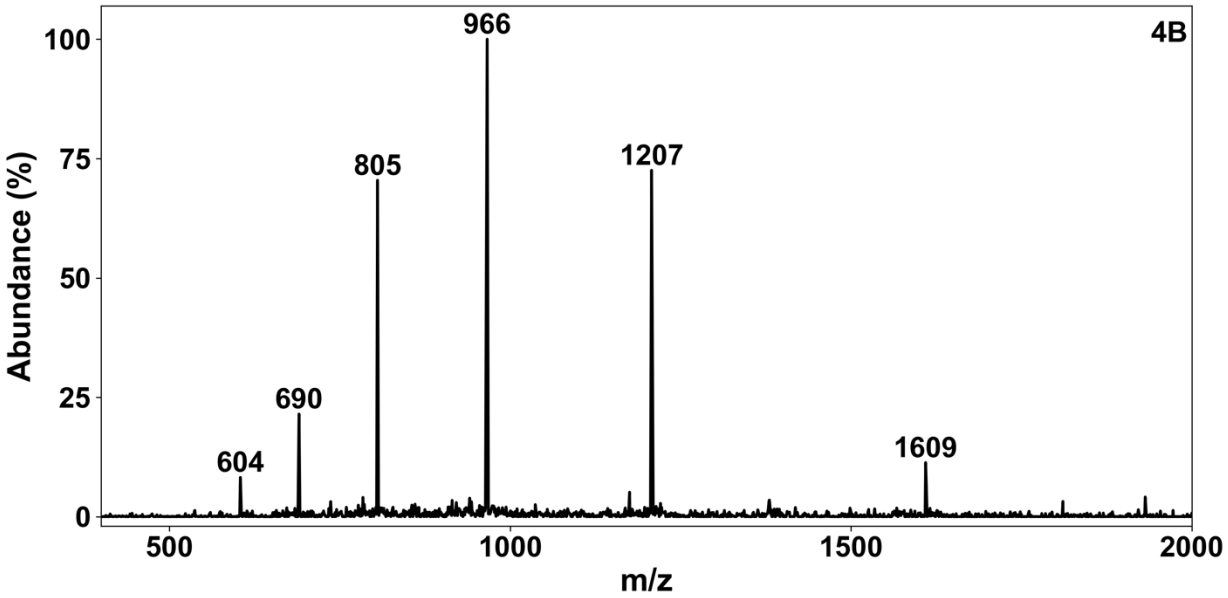

Figure S3. Mass spectrometry data of **4B** peptide. Expected mass: $[M+H]^{+}/1=4828$, $[M+3H]^{3+}/3=1610$, $[M+4H]^{4+}/4=1208$, $[M+5H]^{5+}/5=966$, $[M+6H]^{6+}/6=805$, $[M+7H]^{7+}/7=690$, $[M+8H]^{8+}/8=604$.

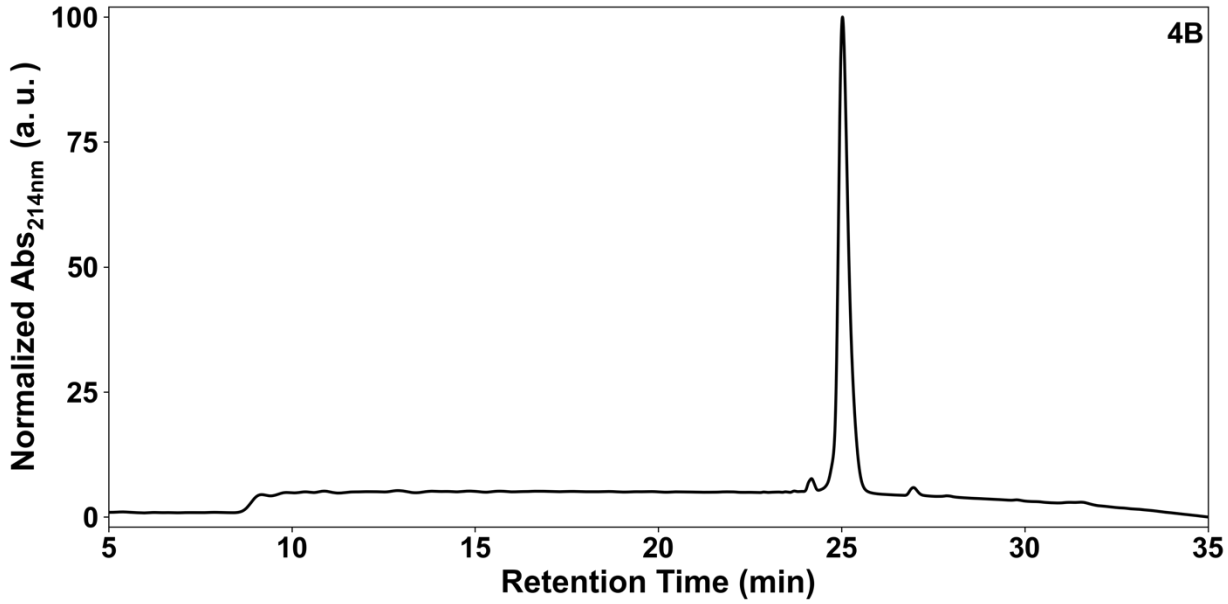

Figure S4. Analytical HPLC trace of the **4B** peptide. A linear gradient of ACN (0.1 vol% TFA) into H_2O (0.1 vol% TFA) over 30 min (5% ACN at 5 min, 95% ACN at 35min) was used.

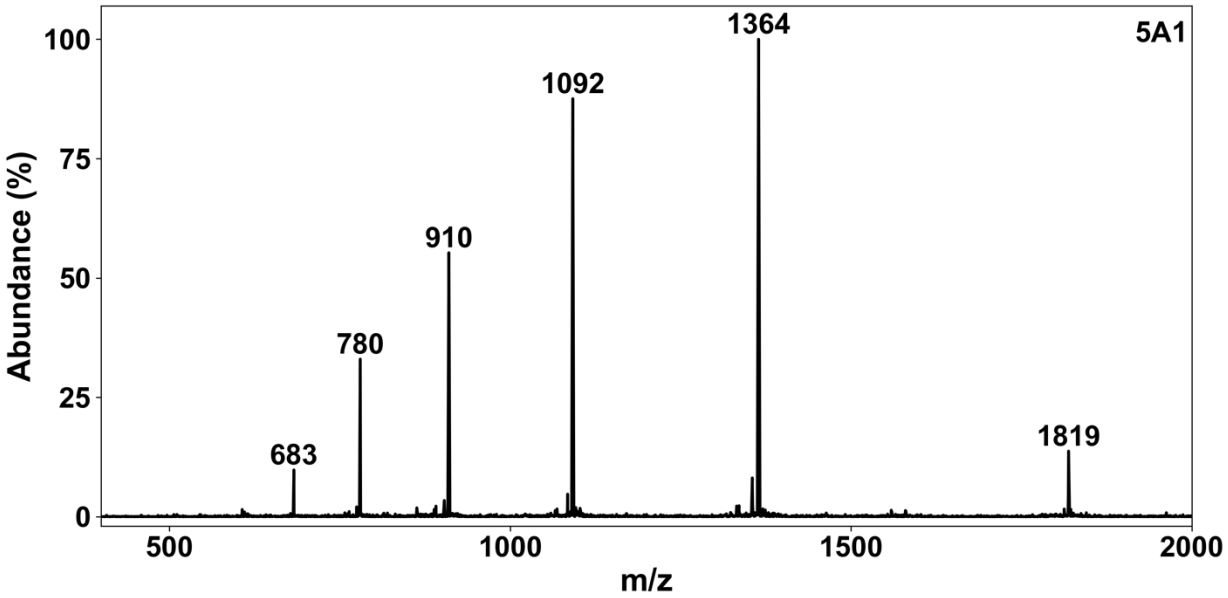

Figure S5. Mass spectrometry data of the **5A1** peptide. Expected mass: $[M+H]^{+}/1=5456$, $[M+3H]^{3+}/3=1819$, $[M+4H]^{4+}/4=1365$, $[M+5H]^{5+}/5=1092$, $[M+6H]^{6+}/6=910$, $[M+7H]^{7+}/7=780$, $[M+8H]^{8+}/8=683$.

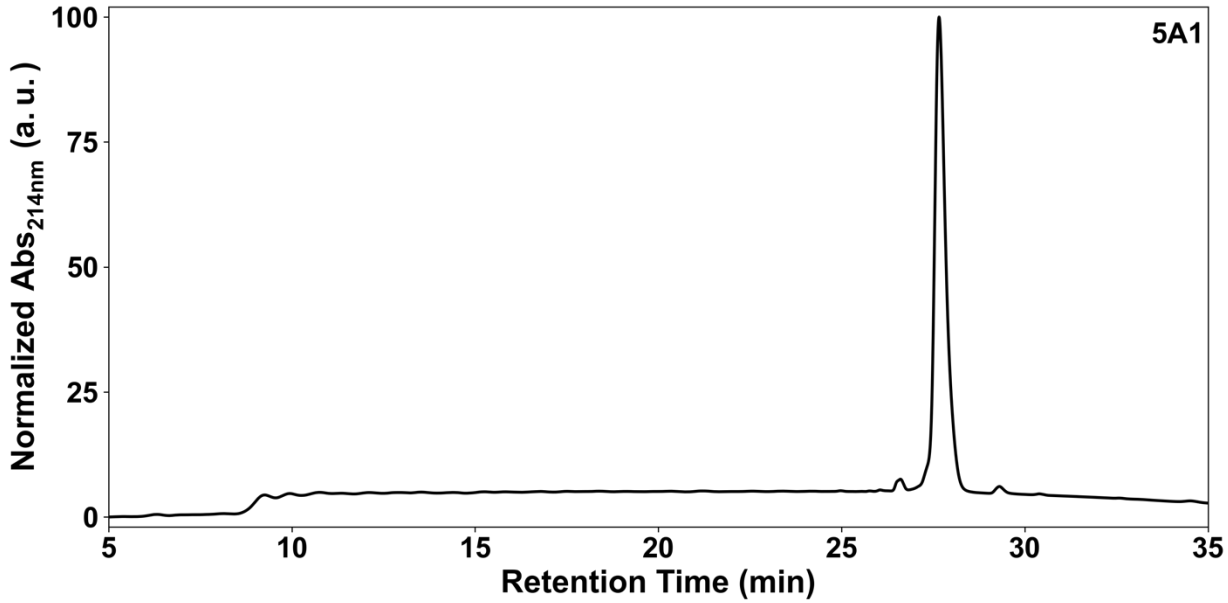

Figure S6. Analytical HPLC trace of the **5A1** peptide. A linear gradient of ACN (0.1 vol% TFA) into H_2O (0.1 vol% TFA) over 30 min (5% ACN at 5 min, 95% ACN at 35min) was used.

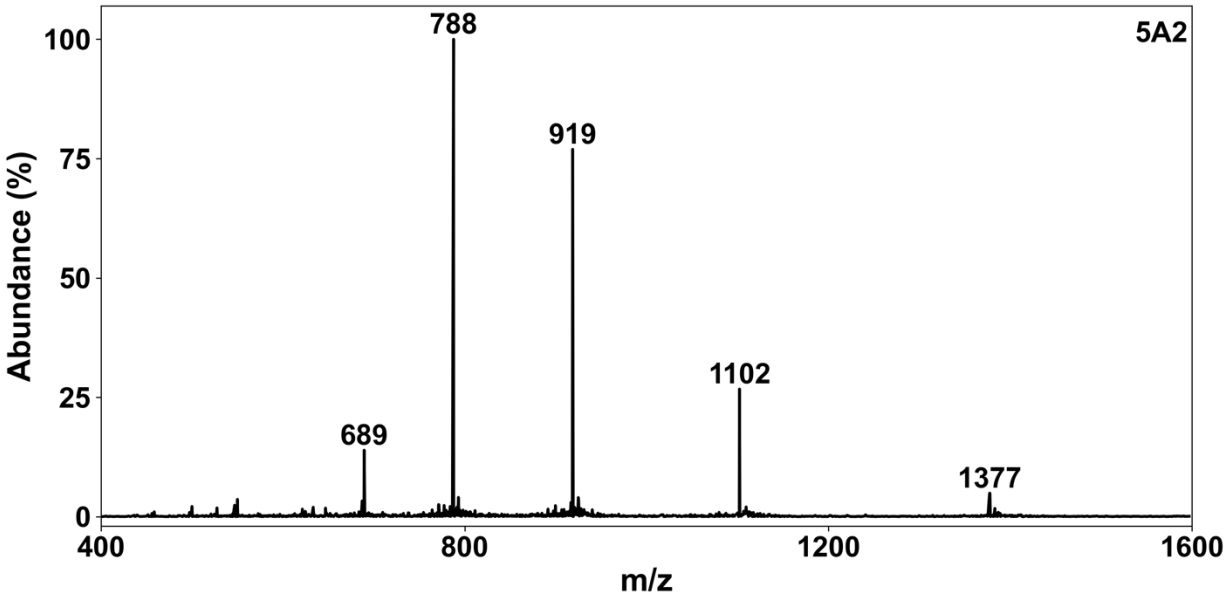

Figure S7. Mass spectrometry data of **5A2** peptide. Expected mass: $[M+H]^{+}/1=5509$, $[M+4H]^{4+}/4=1378$, $[M+5H]^{5+}/5=1103$, $[M+6H]^{6+}/6=919$, $[M+7H]^{7+}/7=788$, $[M+8H]^{88+}/8=689$.

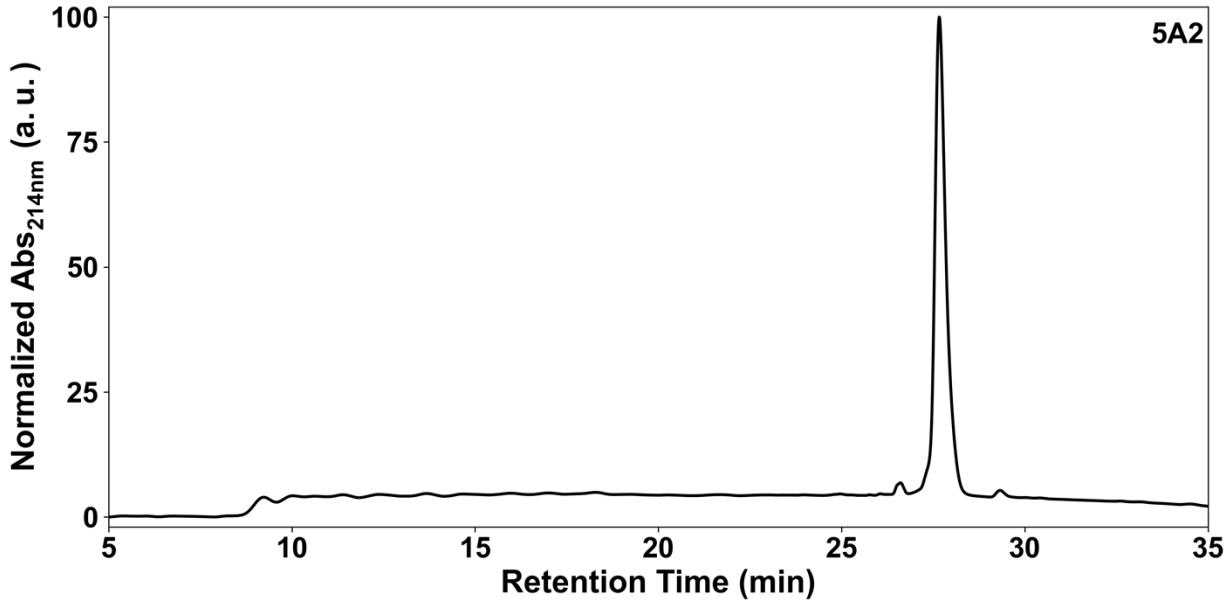

Figure S8. Analytical HPLC trace of **5A2** peptide. A linear gradient of ACN (0.1 vol% TFA) into H_2O (0.1 vol% TFA) over 30 min (5% ACN at 5 min, 95% ACN at 35min) was used.

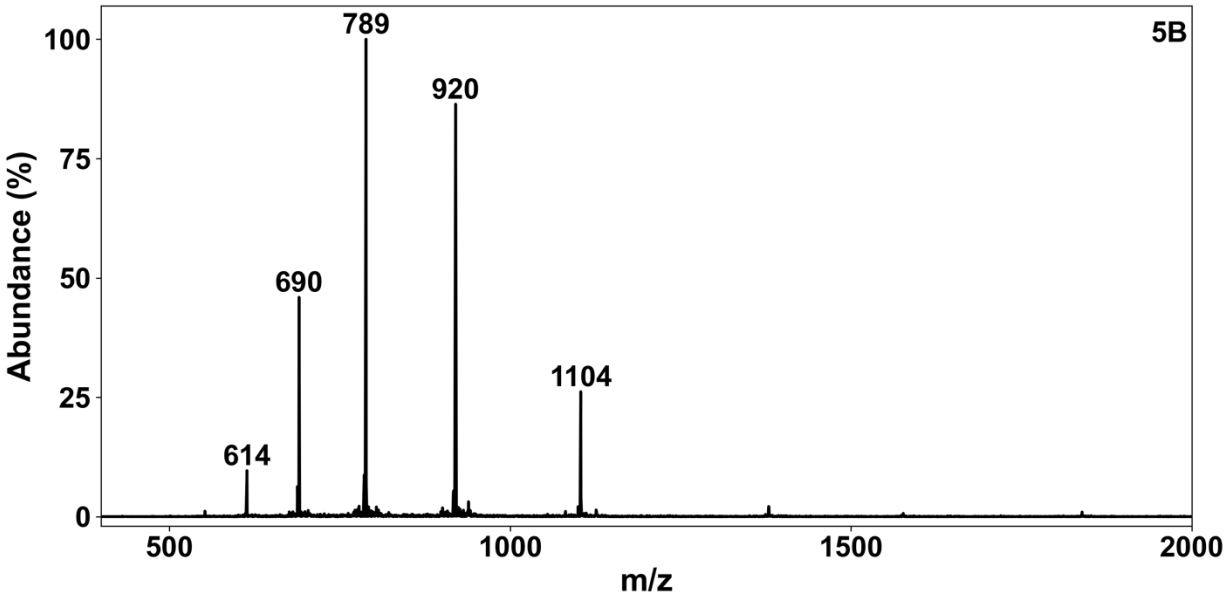

Figure S9. Mass spectrometry data of the **5B** peptide. Expected mass: $[M+H]^{+}/1=5518$, $[M+5H]^{5+}/5=1104$, $[M+6H]^{6+}/6=921$, $[M+7H]^{7+}/7=789$, $[M+8H]^{8+}/8=691$, $[M+9H]^{9+}/9=614$.

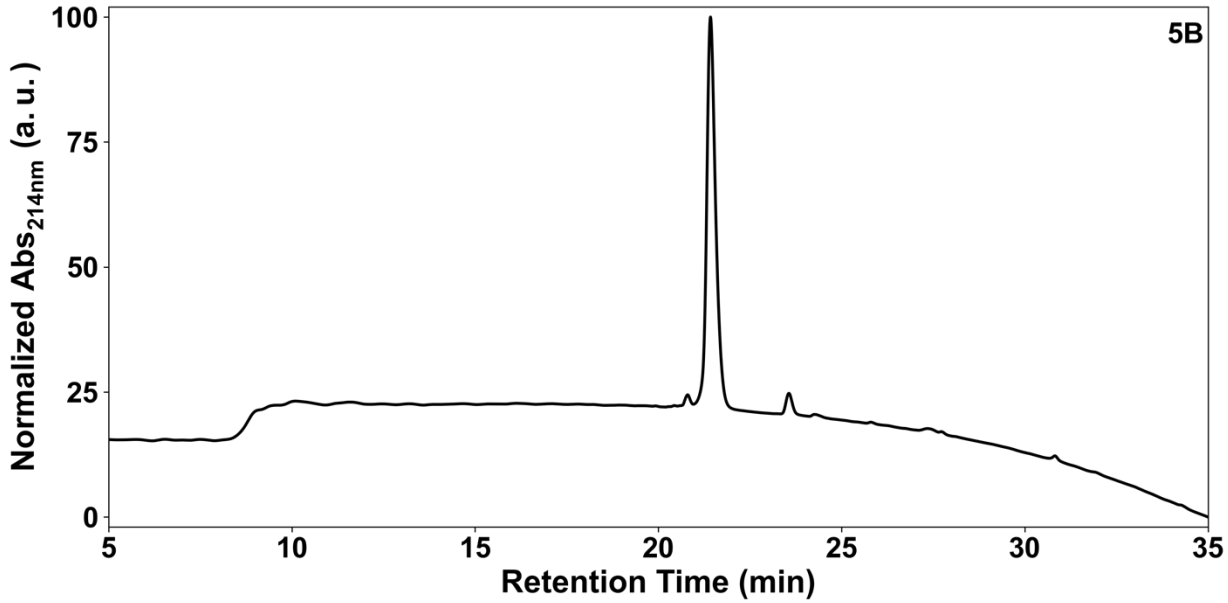

Figure S10. Analytical HPLC trace of the **5B** peptide. A linear gradient of ACN (0.1 vol% TFA) into H_2O (0.1 vol% TFA) over 30 min (5% ACN at 5 min, 95% ACN at 35min) was used.

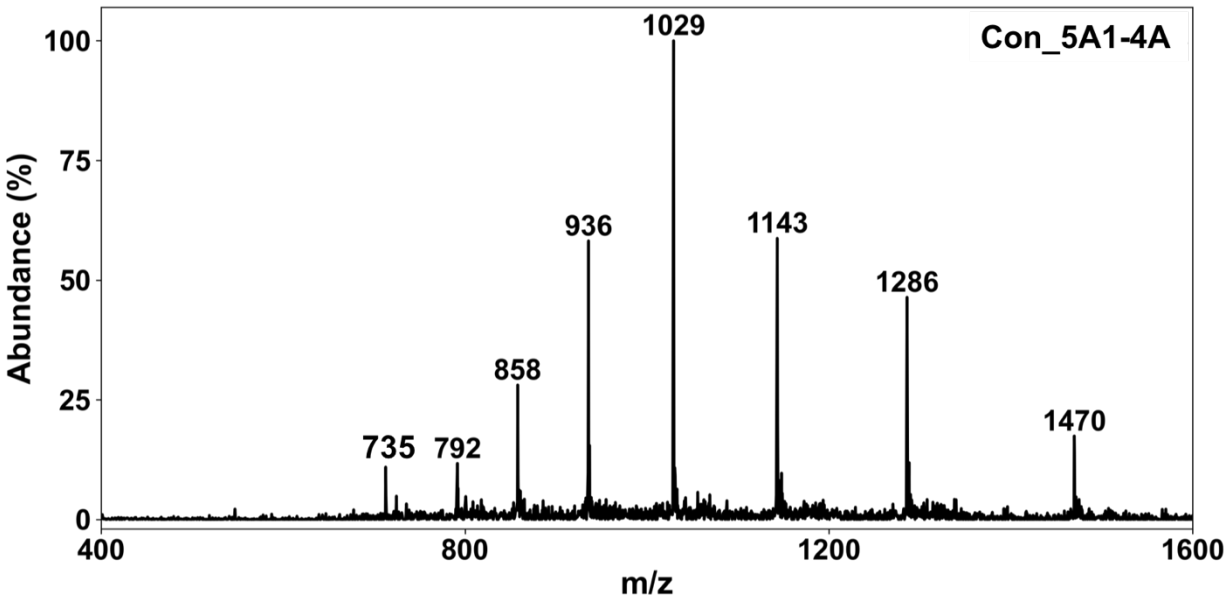

Figure S11. Mass spectrometry data of **Con_5A1-4A**. Expected mass: $[M+H]^{+}/1=10287$, $[M+7H]^{7+}/7=1470$, $[M+8H]^{8+}/8=1287$, $[M+9H]^{9+}/9=1144$, $[M+10H]^{10+}/10=1030$, $[M+11H]^{11+}/11=936$, $[M+12H]^{12+}/12=858$, $[M+13H]^{13+}/13=792$, $[M+14H]^{14+}/14=736$.

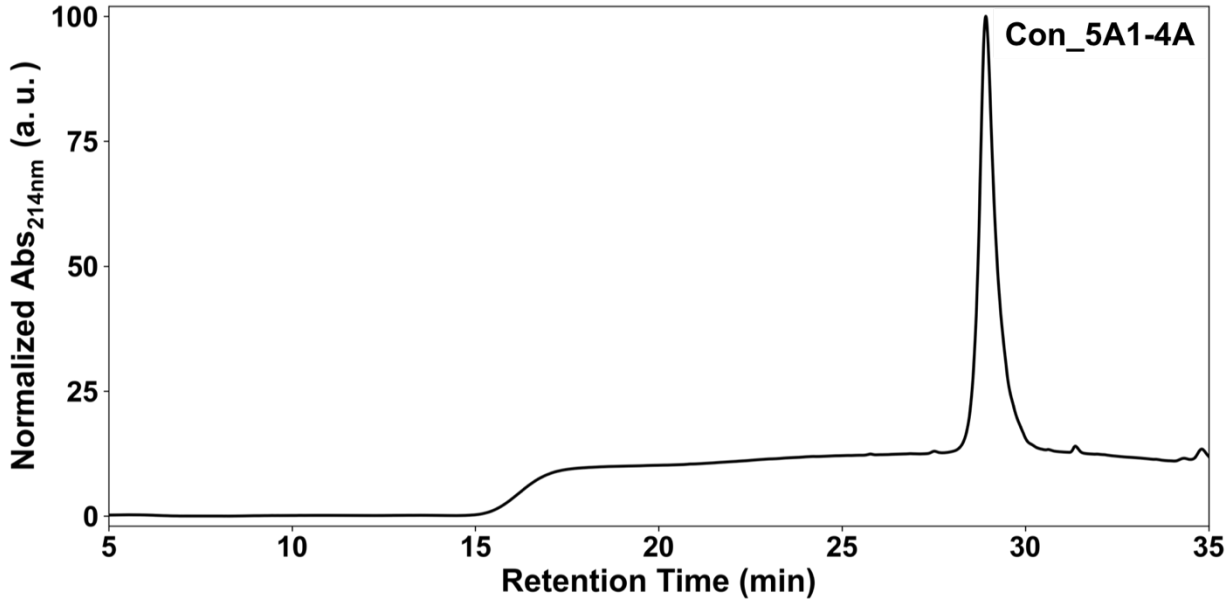

Figure S12. Analytical HPLC trace of **Con_5A1-4A**. A linear gradient of ACN (0.1 vol% TFA) into H_2O (0.1 vol% TFA) over 30 min (5% ACN at 5 min, 95% ACN at 35min) was used.

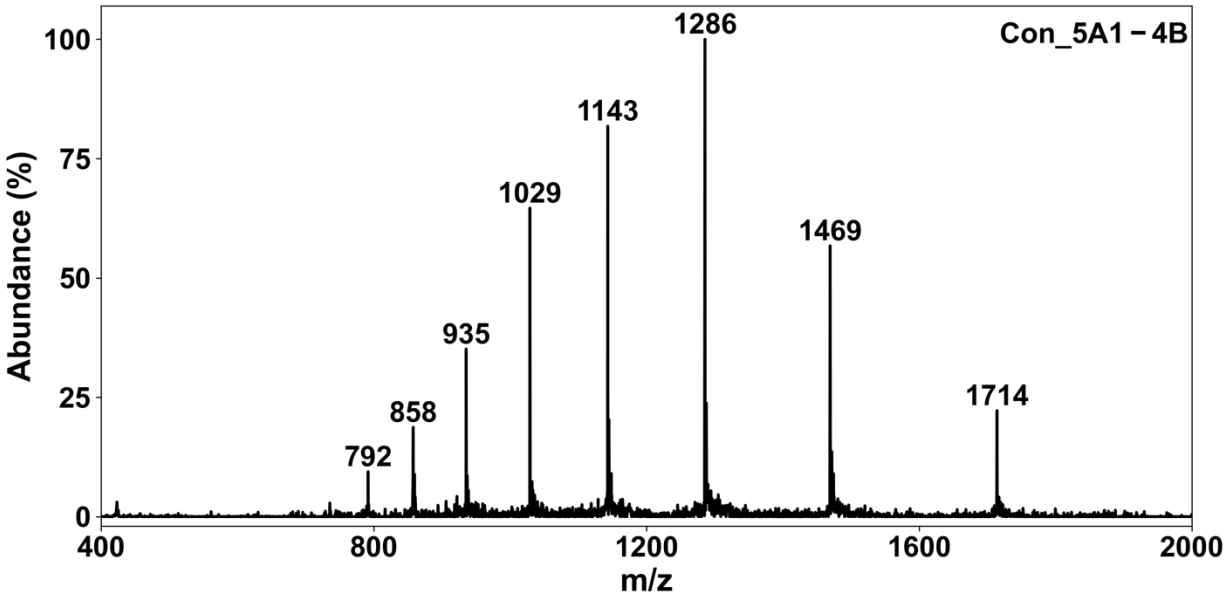

Figure S13. Mass spectrometry data of **Con_5A1-4B**. Expected mass: $[M+H]^{+}/1=10283$, $[M+6H]^{6+}/6=1715$, $[M+7H]^{7+}/7=1470$, $[M+8H]^{8+}/8=1286$, $[M+9H]^{9+}/9=1143$, $[M+10H]^{10+}/10=1029$, $[M+11H]^{11+}/11=936$, $[M+12H]^{12+}/12=858$, $[M+13H]^{13+}/13=792$.

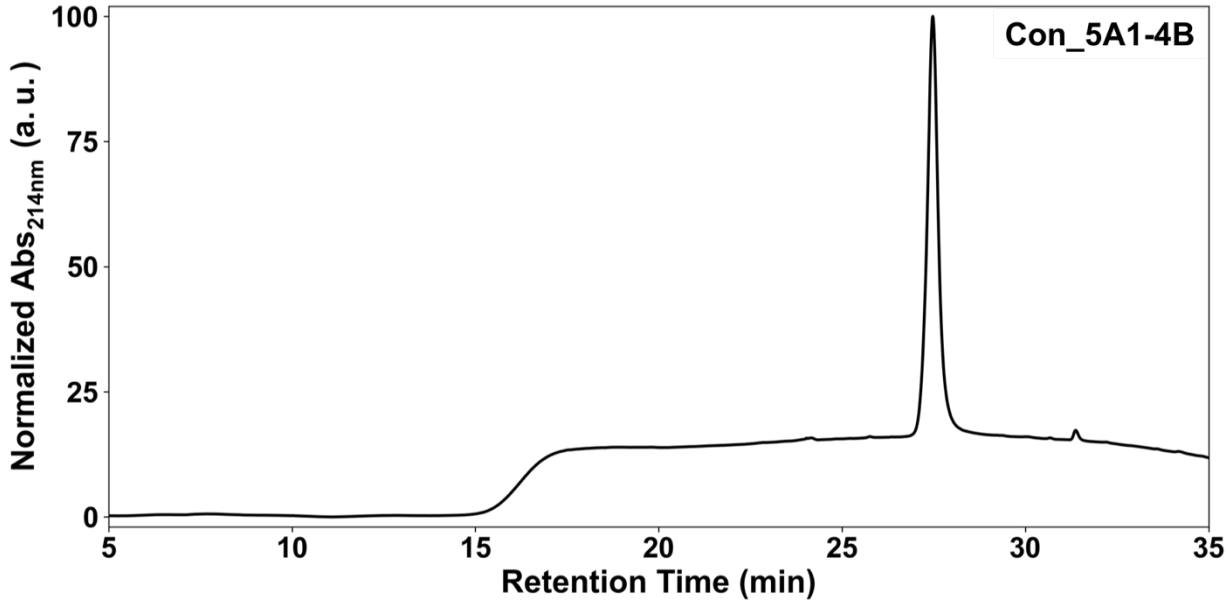

Figure S14. Analytical HPLC trace of **Con_5A1-4B**. A linear gradient of ACN (0.1 vol% TFA) into H_2O (0.1 vol% TFA) over 30 min (5% ACN at 5 min, 95% ACN at 35min) was used.

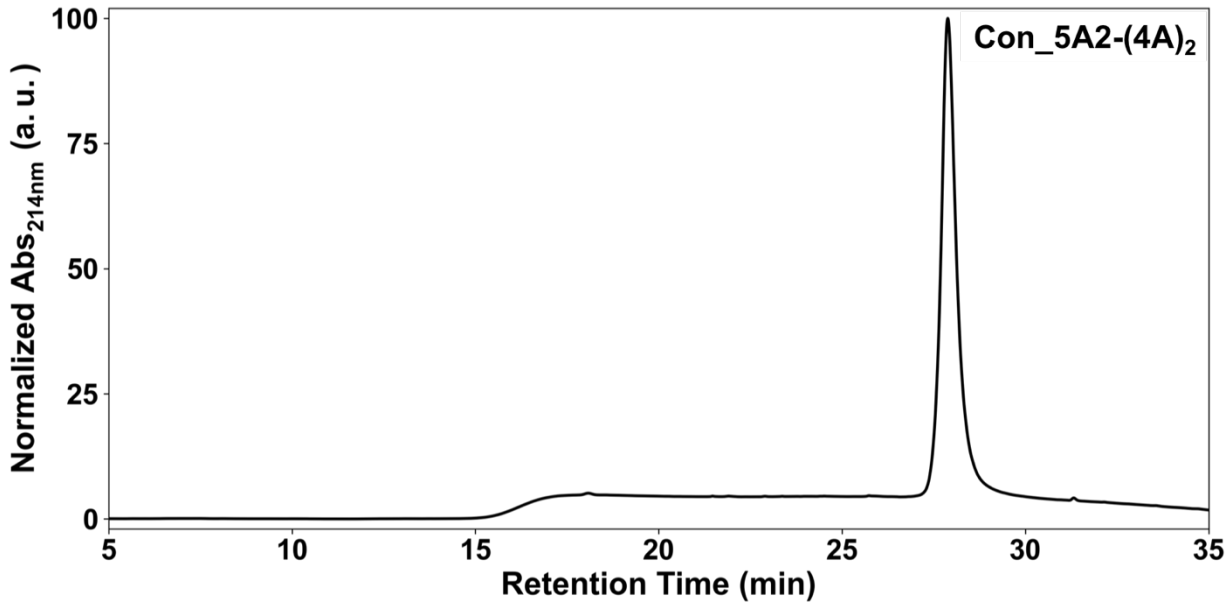

Figure S15. Analytical HPLC trace of **Con_5A2-(4A)$_2$**. A linear gradient of ACN (0.1 vol% TFA) into H_2O (0.1 vol% TFA) over 30 min (5% ACN at 5 min, 95% ACN at 35min) was used.

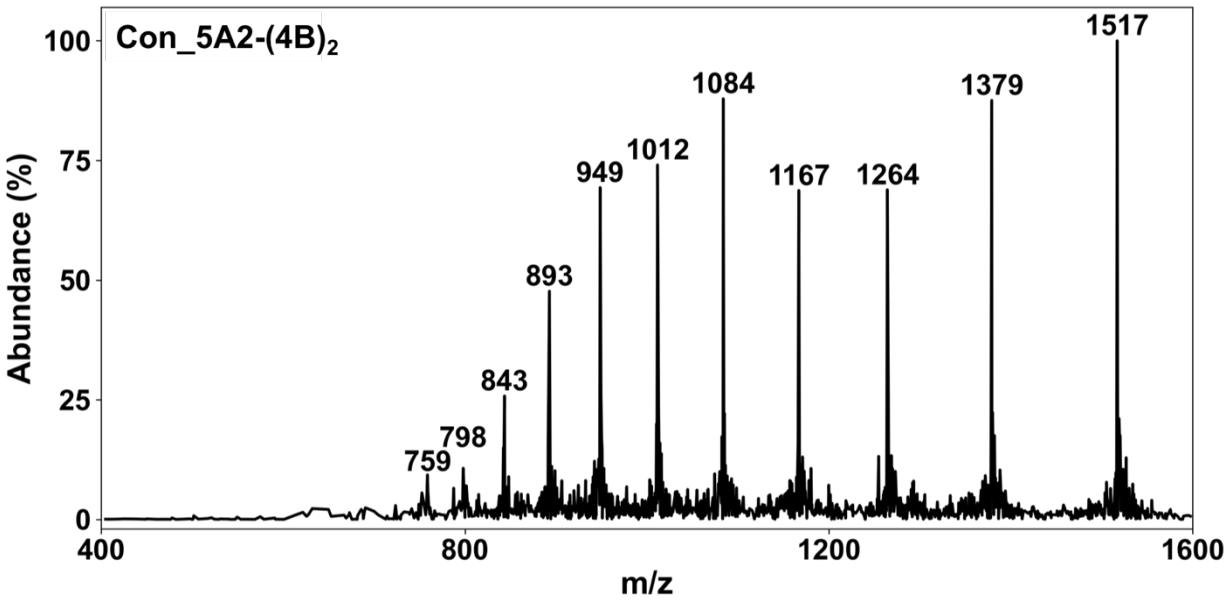

Figure S16. Mass spectrometry data of **Con_5A2-(4B)$_2$**. Expected mass: $[M+H]^{+}/1=15163$, $[M+10H]^{10+}/10=1517$, $[M+11H]^{11+}/11=1379$, $[M+12H]^{12+}/12=1264$, $[M+13H]^{13+}/13=1167$, $[M+14H]^{14+}/14=1084$, $[M+15H]^{15+}/15=1012$, $[M+16H]^{16+}/16=949$, $[M+17H]^{17+}/17=893$, $[M+18H]^{18+}/18=843$, $[M+19H]^{19+}/19=799$, $[M+20H]^{20+}/20=759$.

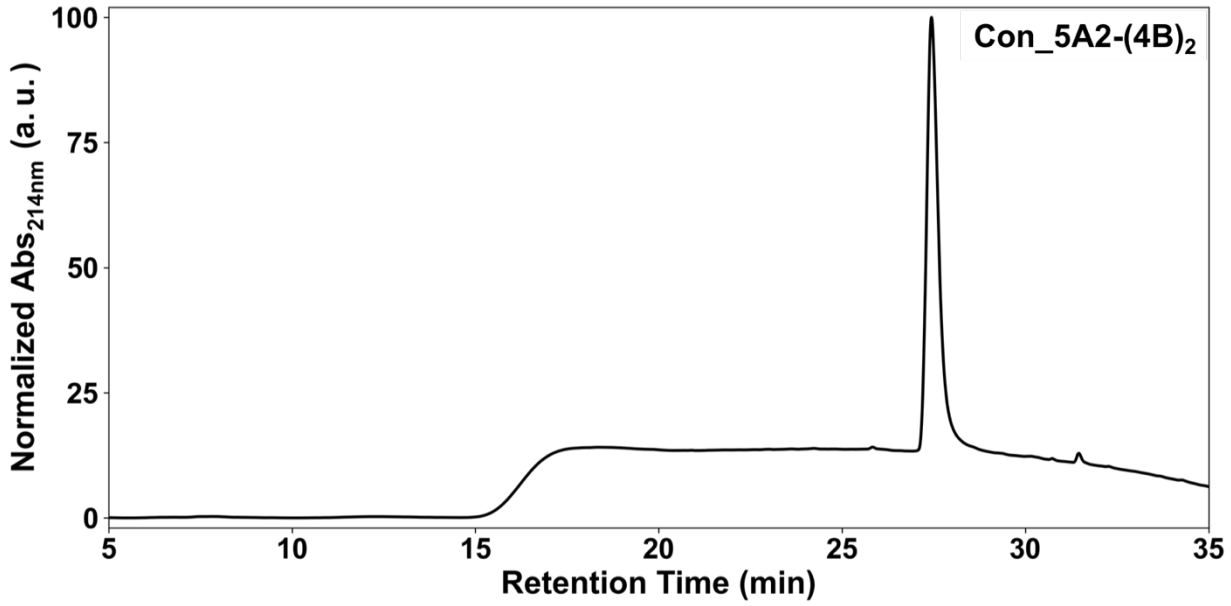

Figure S17. Analytical HPLC trace of **Con_5A2-(4B)$_2$**. A linear gradient of ACN (0.1 vol% TFA) into H_2O (0.1 vol% TFA) over 30 min (5% ACN at 5 min, 95% ACN at 35min) was used.

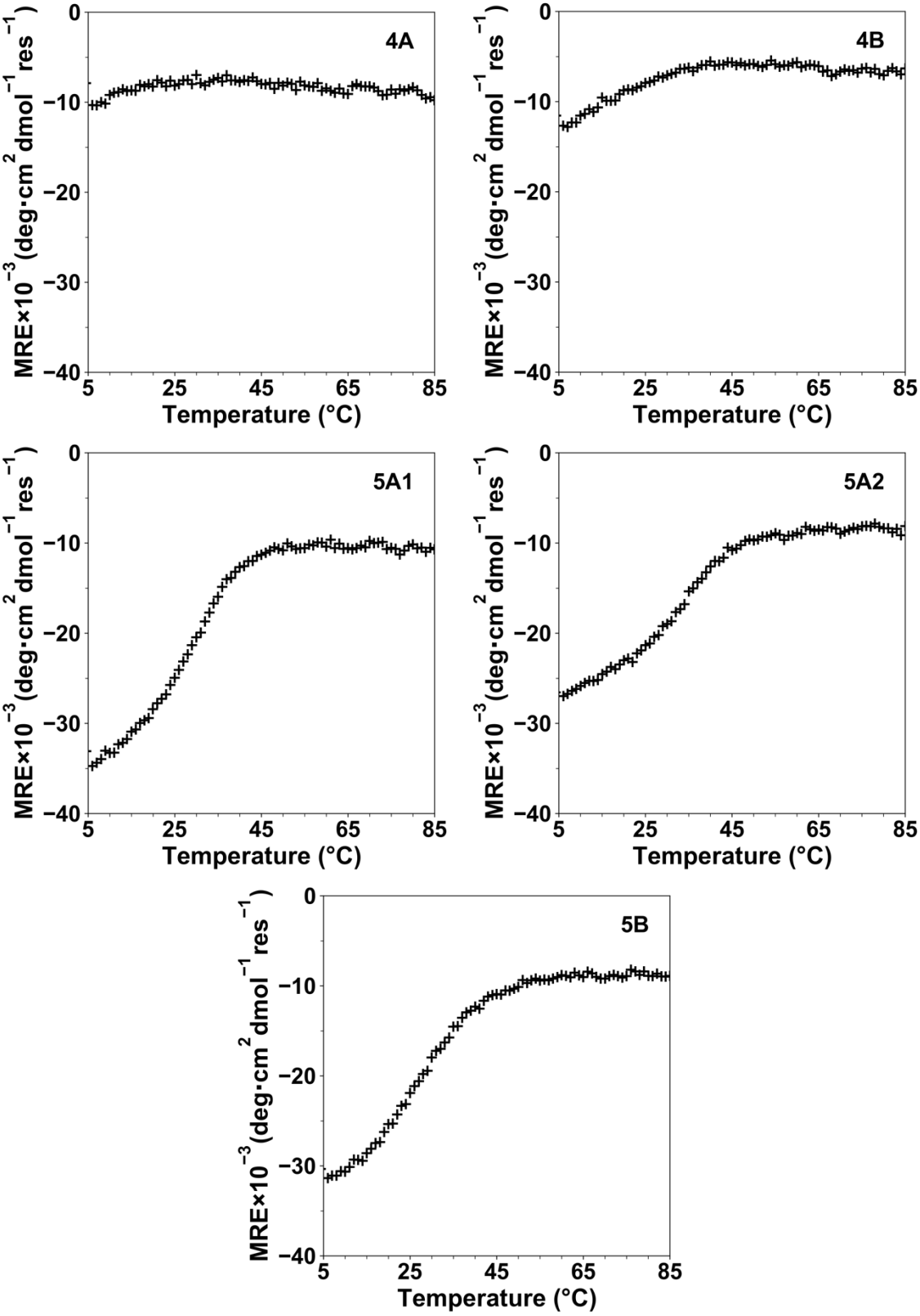
4A
4B
5A1
5A2
5B
MRE×10^{-3}(deg·cm^{2}dmol^{-1}res^{-1})
Temperature (°C)
0
−10
−20
−30
−40
5
25
45
65
85

Figure S18. Thermal denaturation profies of individual single-chain peptides, as monitored by Circular Dichroism at 222 nm. Peptide concentration: 0.01 mM; solvent: 12.5 mM potassium phosphate-150 mM potassium chloride buffer, pH 7.5.

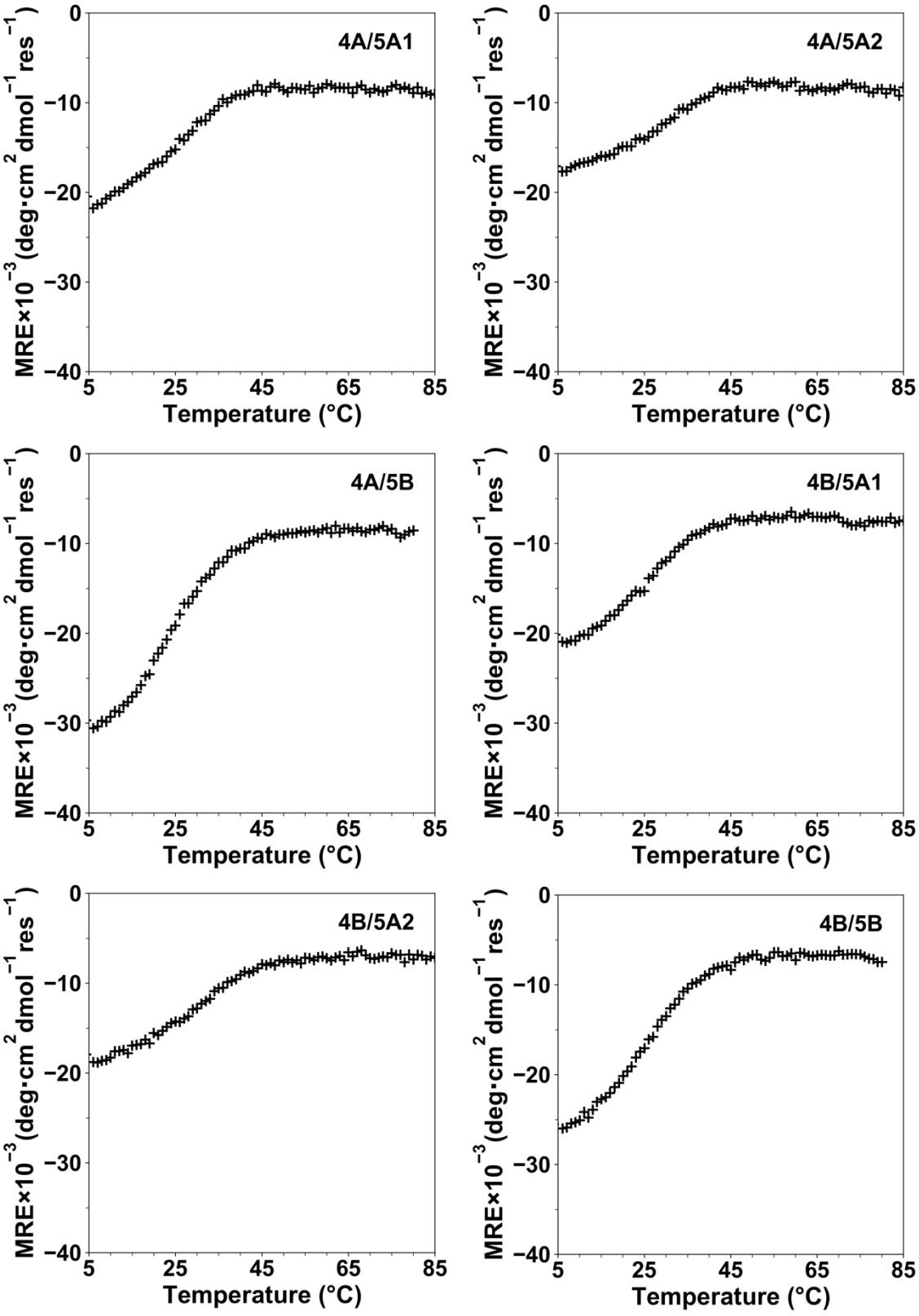

Figure S19. Thermal denaturation profies of equimolar mixtures of non-complementary peptide pairs, as monitored by Circular Dichroism at 222 nm. Total peptide concentration: 0.01 mM; solvent: 12.5 mM potassium phosphate-150 mM potassium chloride buffer, pH 7.5.

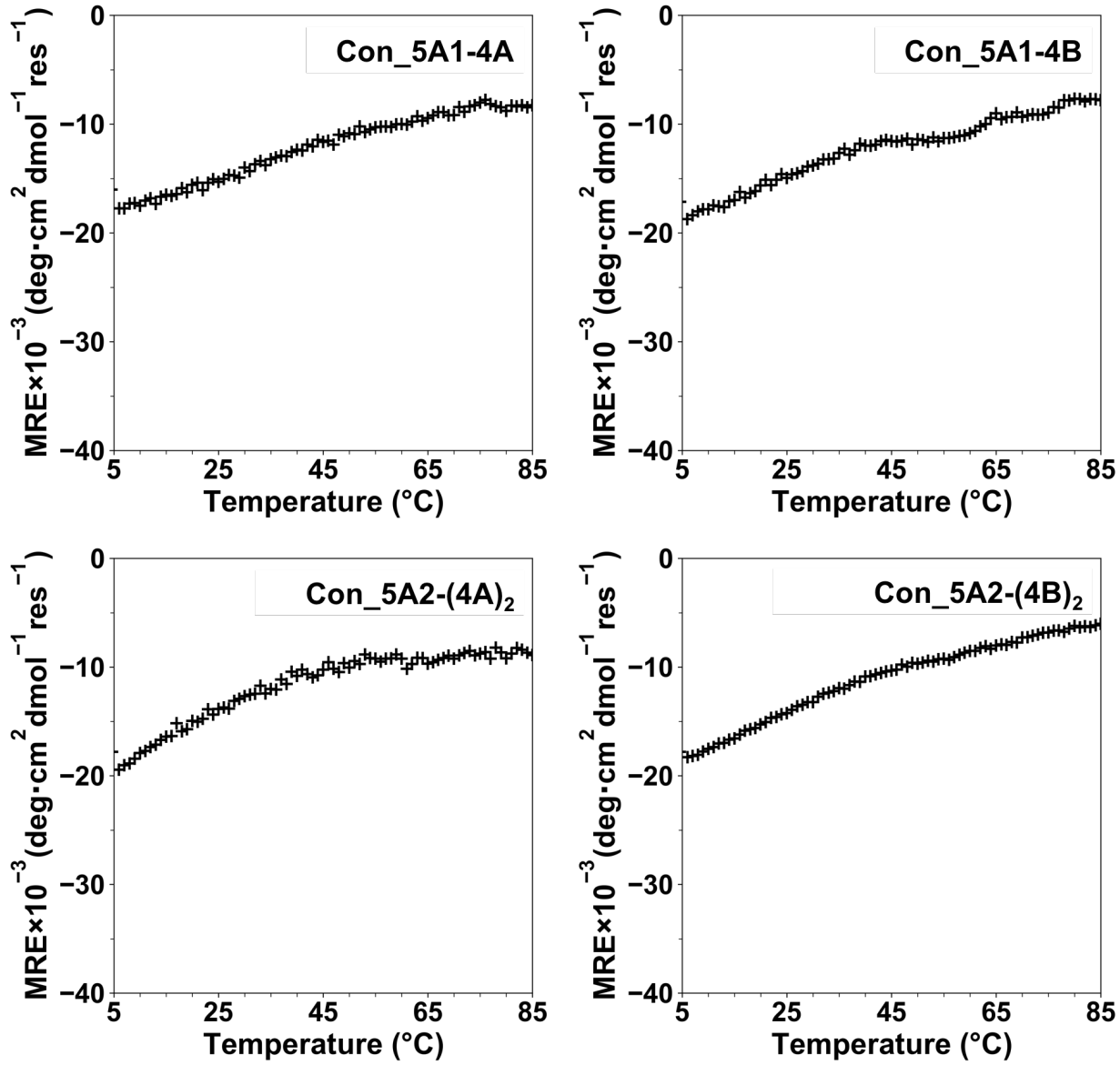

Figure S20. Thermal denaturation profies of conjugated peptides, as monitored by Circular Dichroism at 222 nm. Peptide concentration: 0.01 mM; solvent: 12.5 mM potassium phosphate-150 mM potassium chloride buffer, pH 7.5.

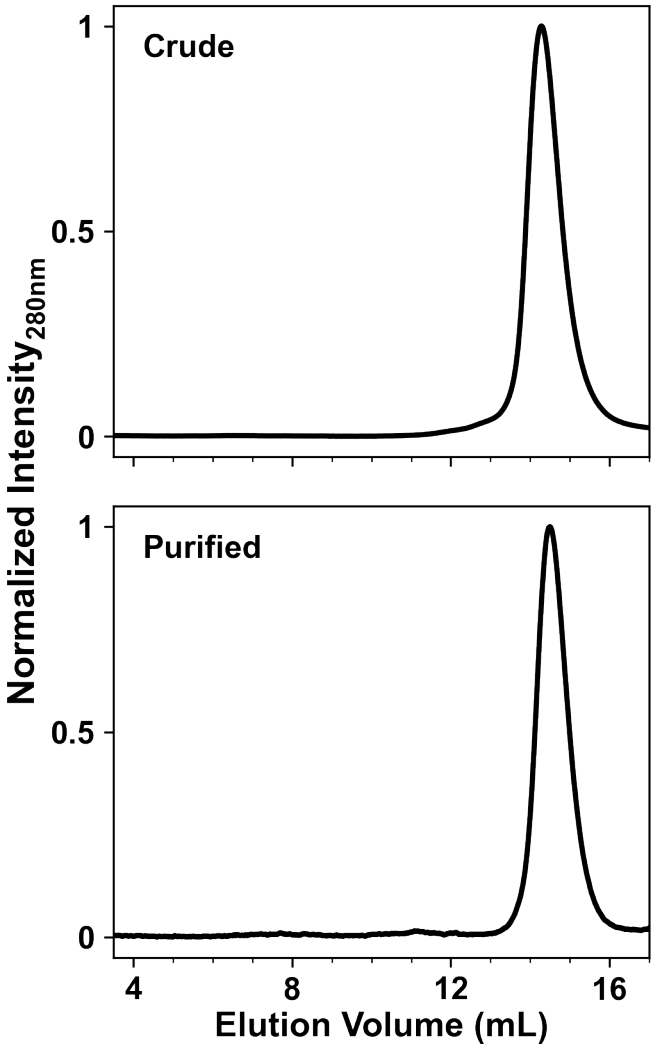

Figure S21. Representative SEC traces of the **4A/4B** dimer before and after SEC purification.

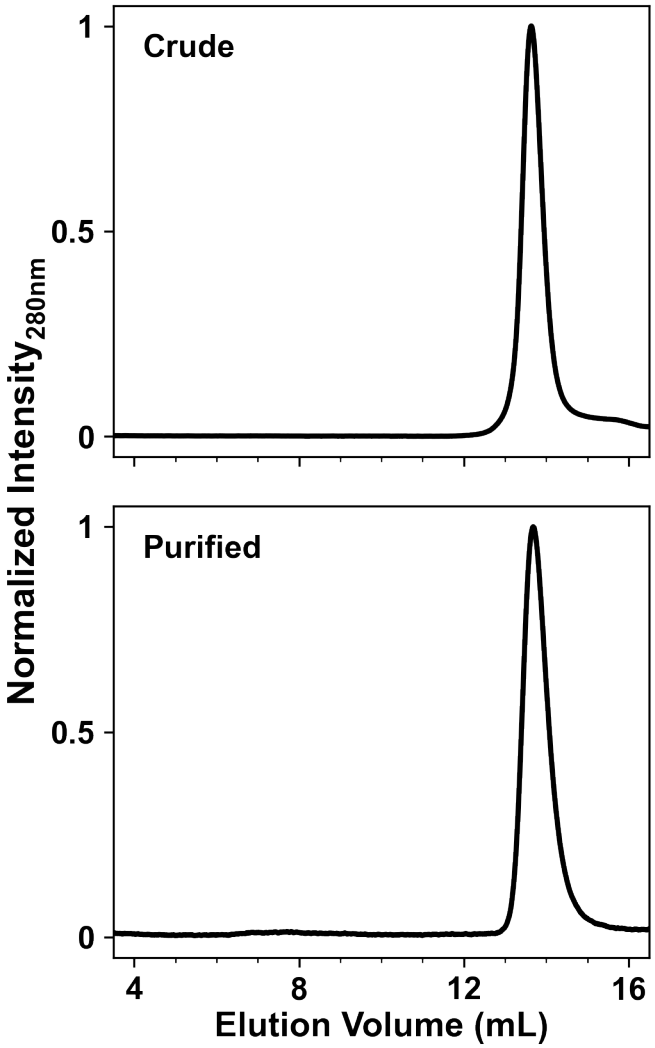

Figure S22. Representative SEC traces of the **5A1/5B** dimer before and after SEC purification.

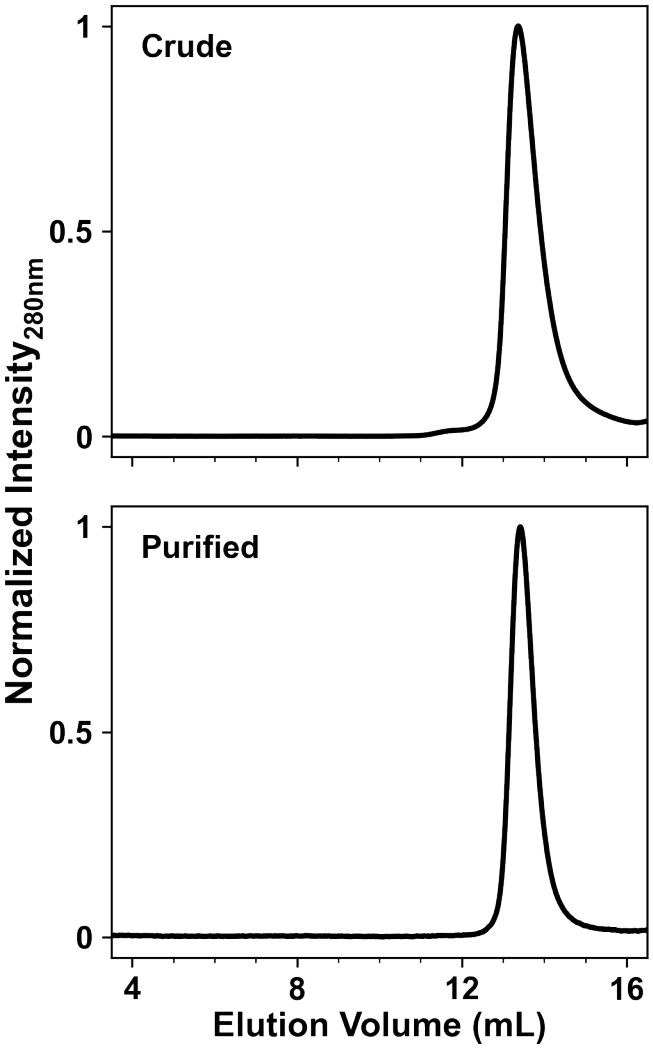

Figure S23. Representative SEC traces of the **5A2/5B** dimer before and after SEC purification.

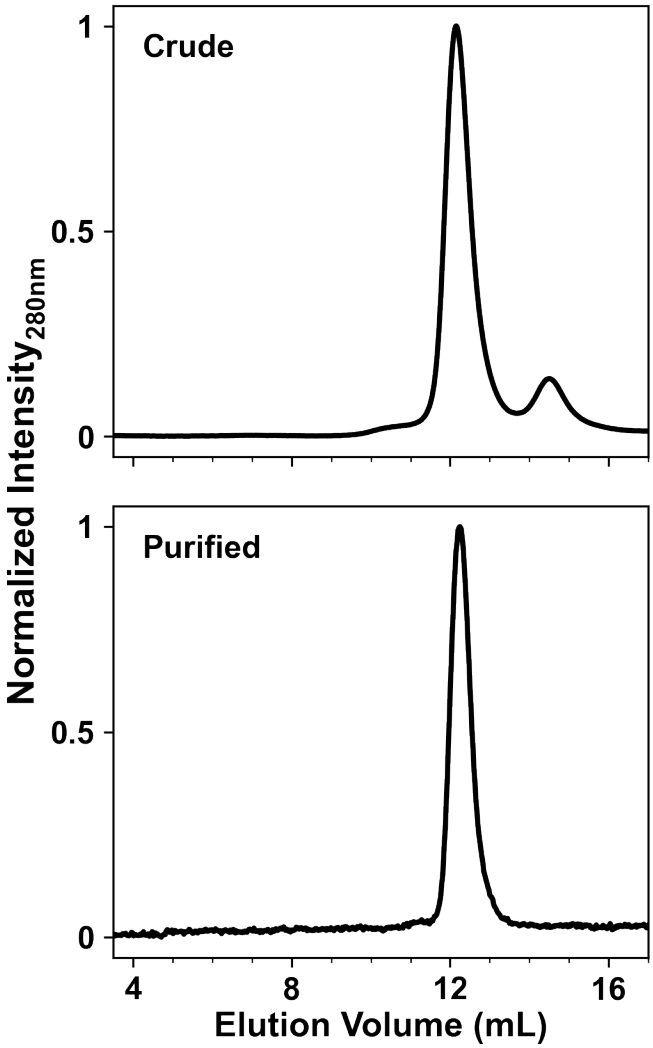

Figure S24. Representative SEC traces of the pre_barbell-A assemblies before and after SEC purification.

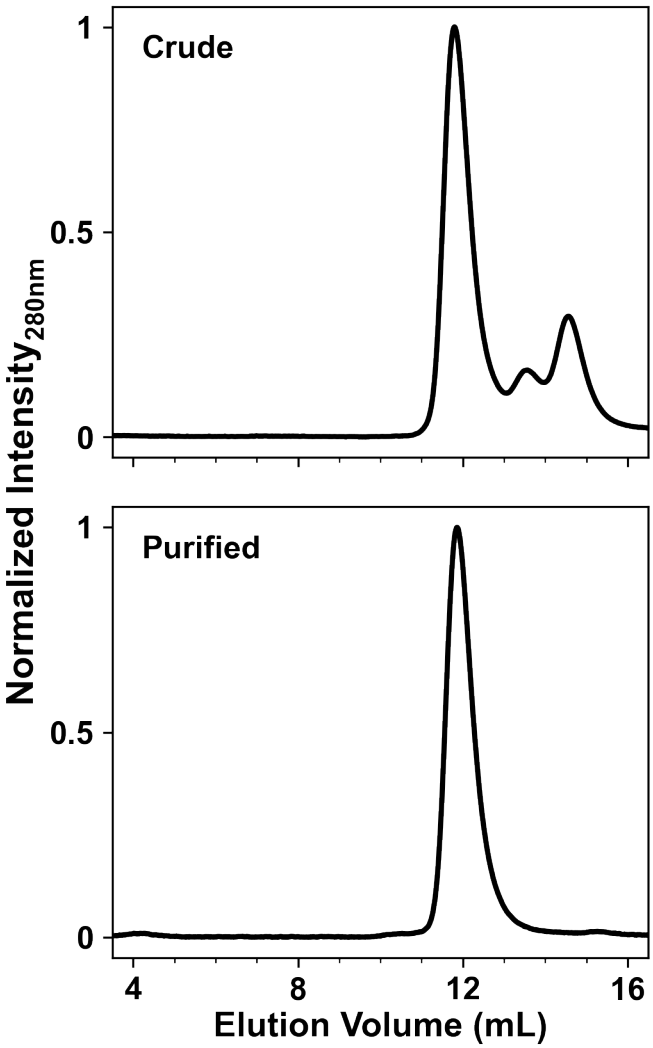

Figure S25. Representative SEC traces of the pre_barbell-B assemblies before and after SEC purification.

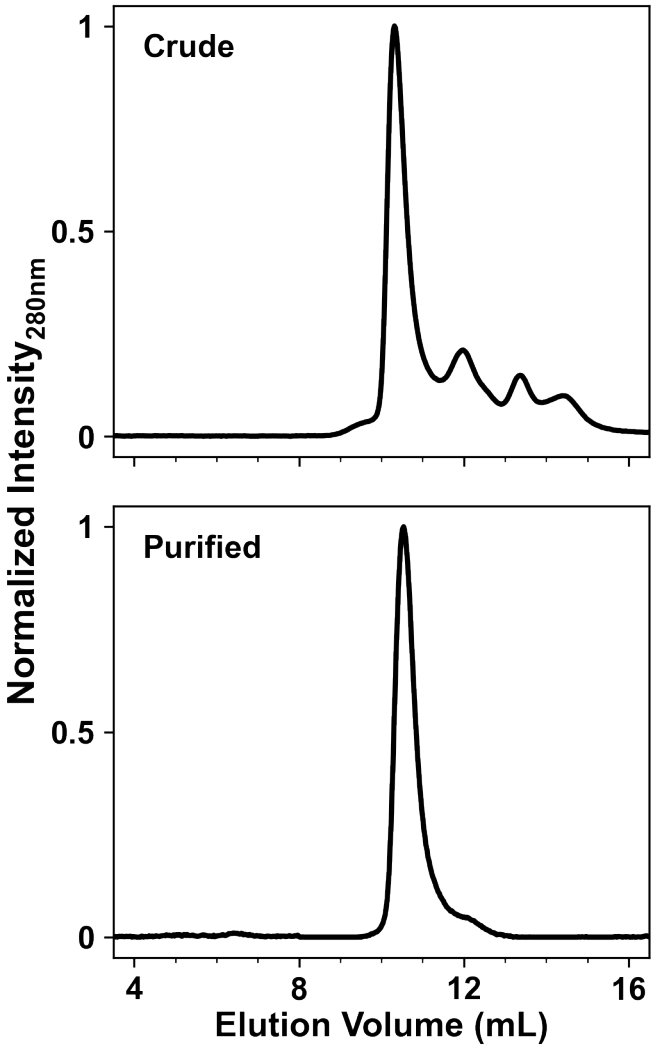

Figure S26. Representative SEC traces of the barbell shaped assemblies before and after SEC purification.

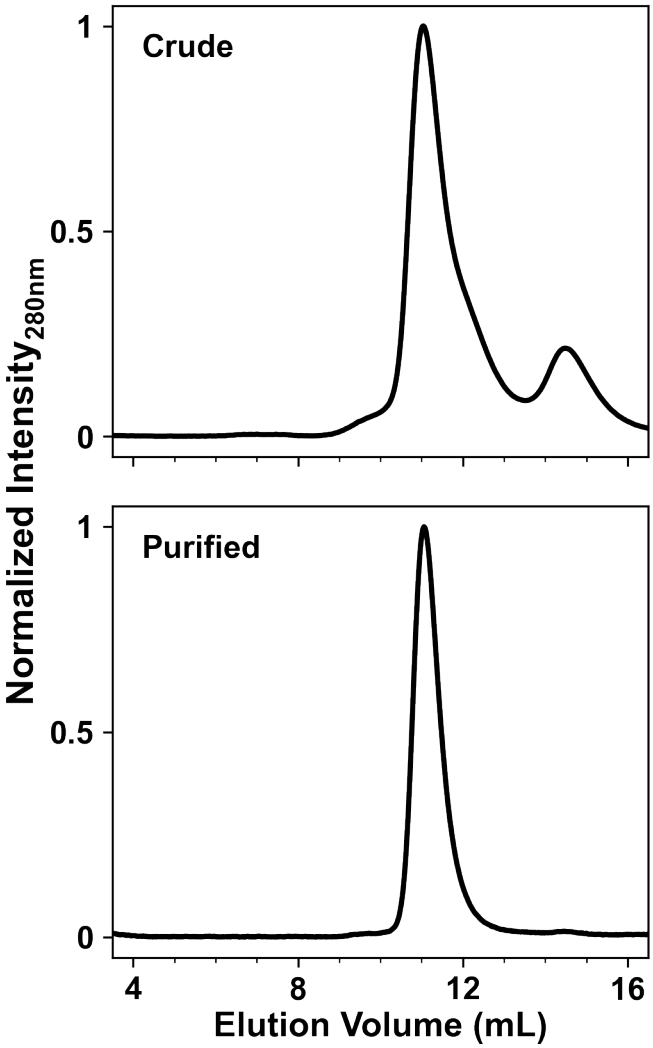

Figure S27. Representative SEC traces of the pre_quadrilateral-A assemblies before and after SEC purification.

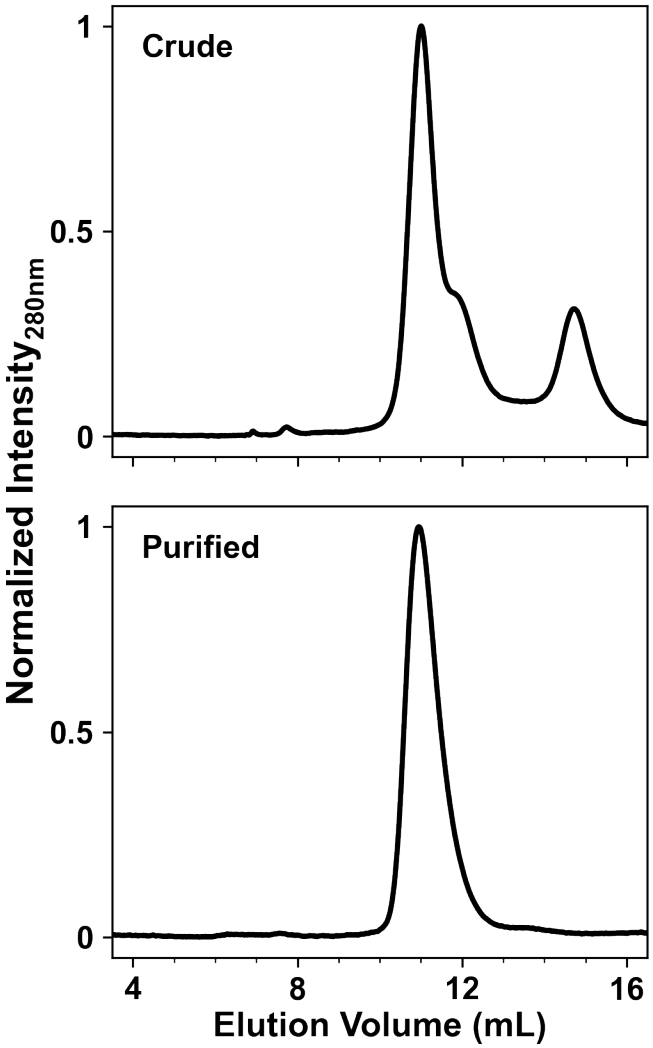

Figure S28. Representative SEC traces of the pre_quadrilateral-B assemblies before and after SEC purification.

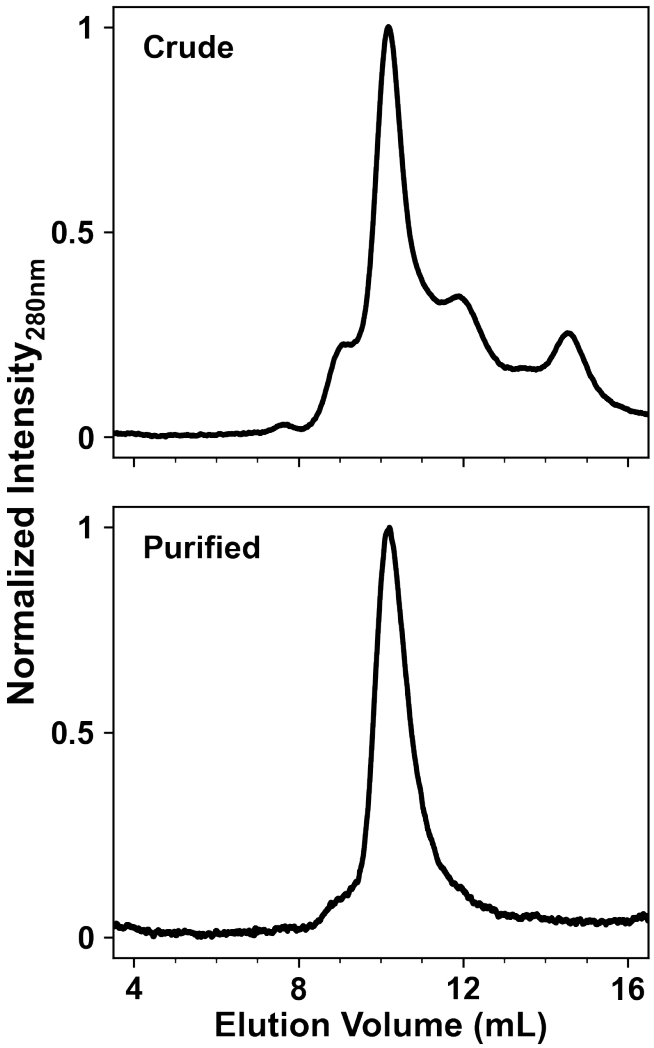

Figure S29. Representative SEC traces of the quadrilateral shaped assemblies before and after SEC purification.

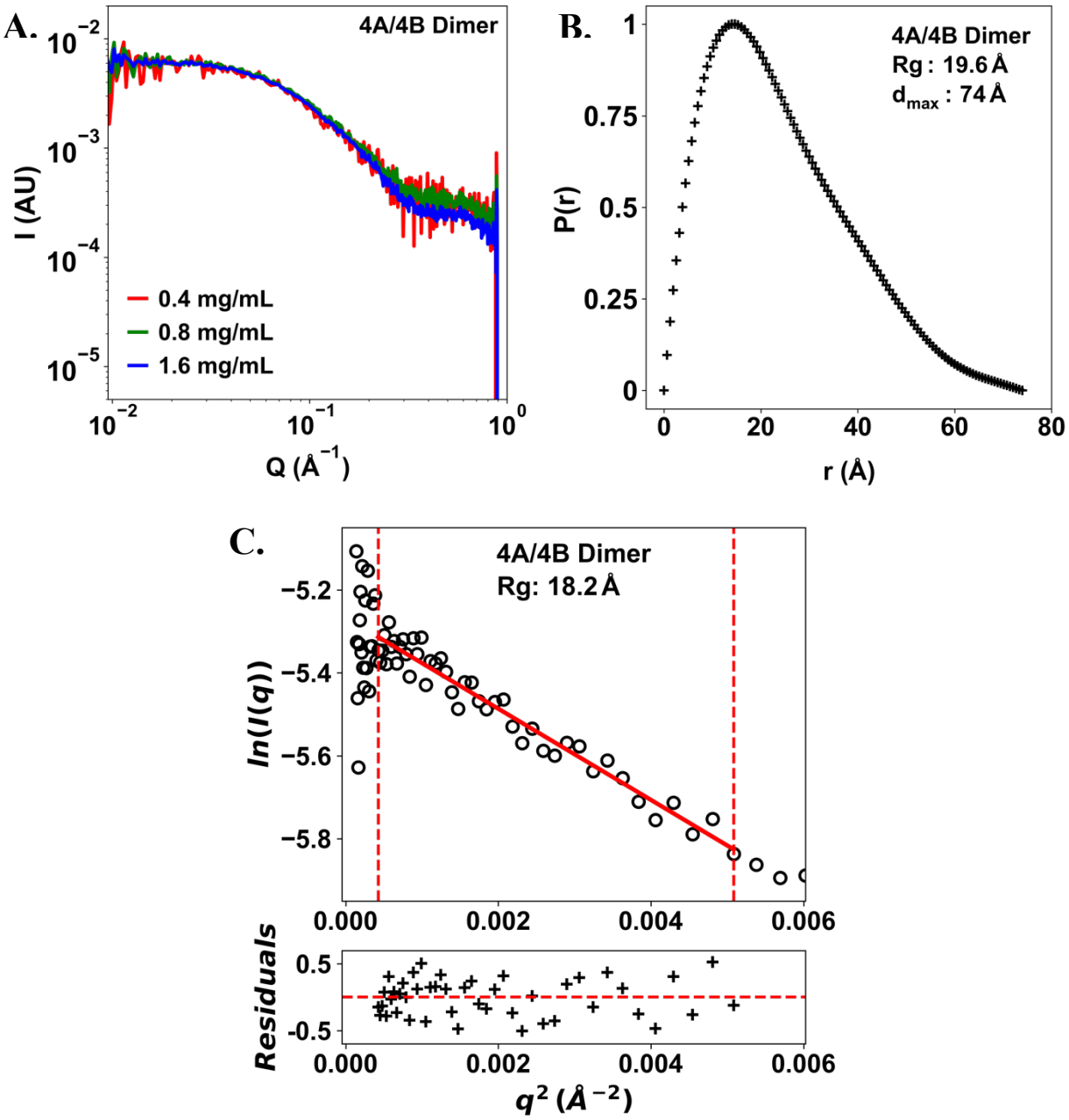

Figure S30. (A) SAXS profiles of the **4A/4B** dimer at various concentrations. (B) The pair-distance distribution function (PDDF) and (C) the Guinier analysis of the **4A/4B** dimer using the SAXS data collected at the concentration of 1.6 mg/mL. No significant structure factor effect was observed in the concentration series. SAXS data of 0.8 mg/ml was chosen for PDDF and Guinier analysis due to its good signal-to-noise ratio and random distribution of residuals from linear fitting. The same reason was used for choosing SAXS data for other samples.

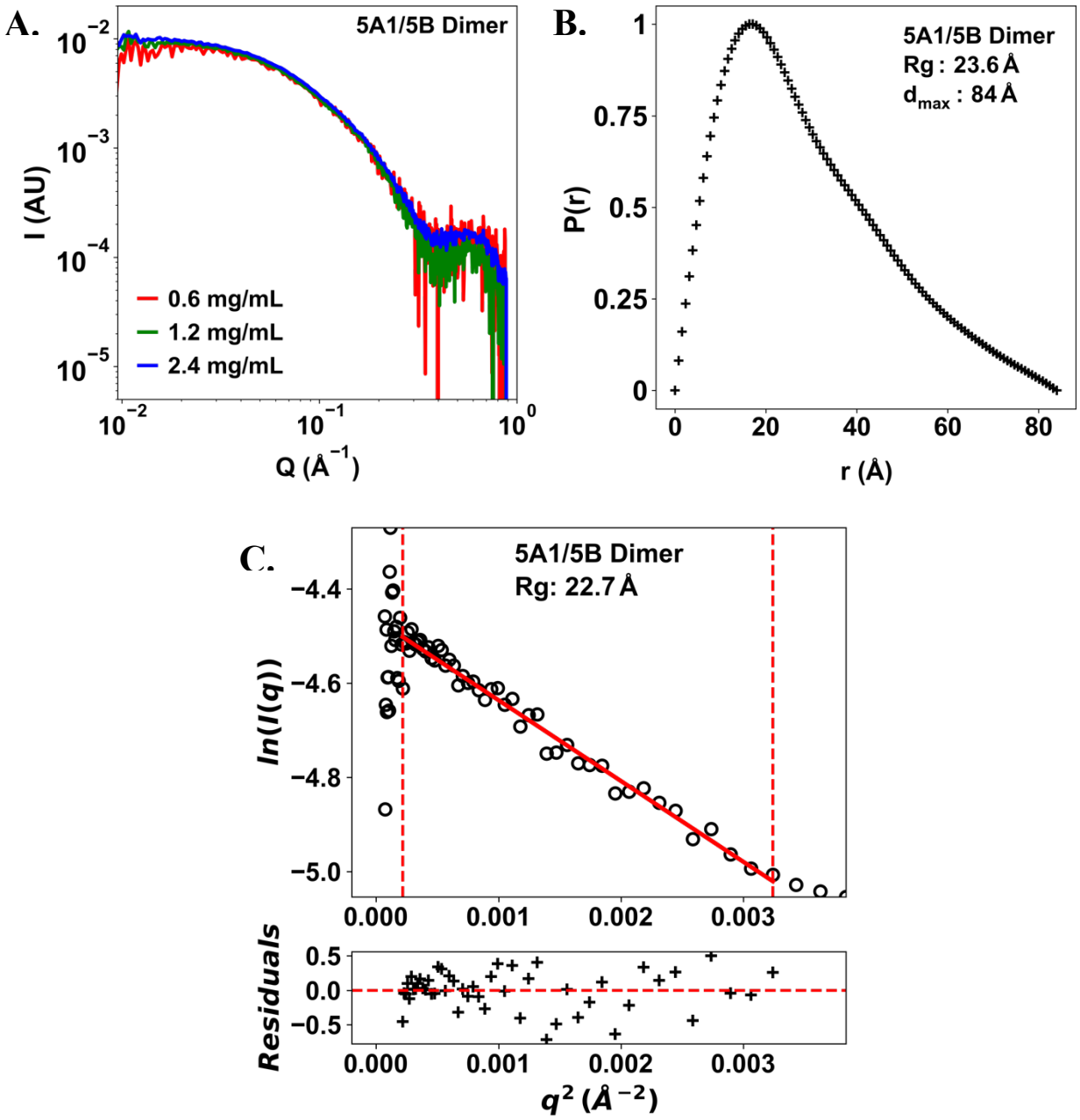

Figure S31. (A) SAXS profiles of the **5A1/5B** dimer at various concentrations. (B) The pair-distance distribution function and (C) the Guinier analysis of the **5A1/5B** dimer using the SAXS data collected at the concentration of 1.2 mg/mL.

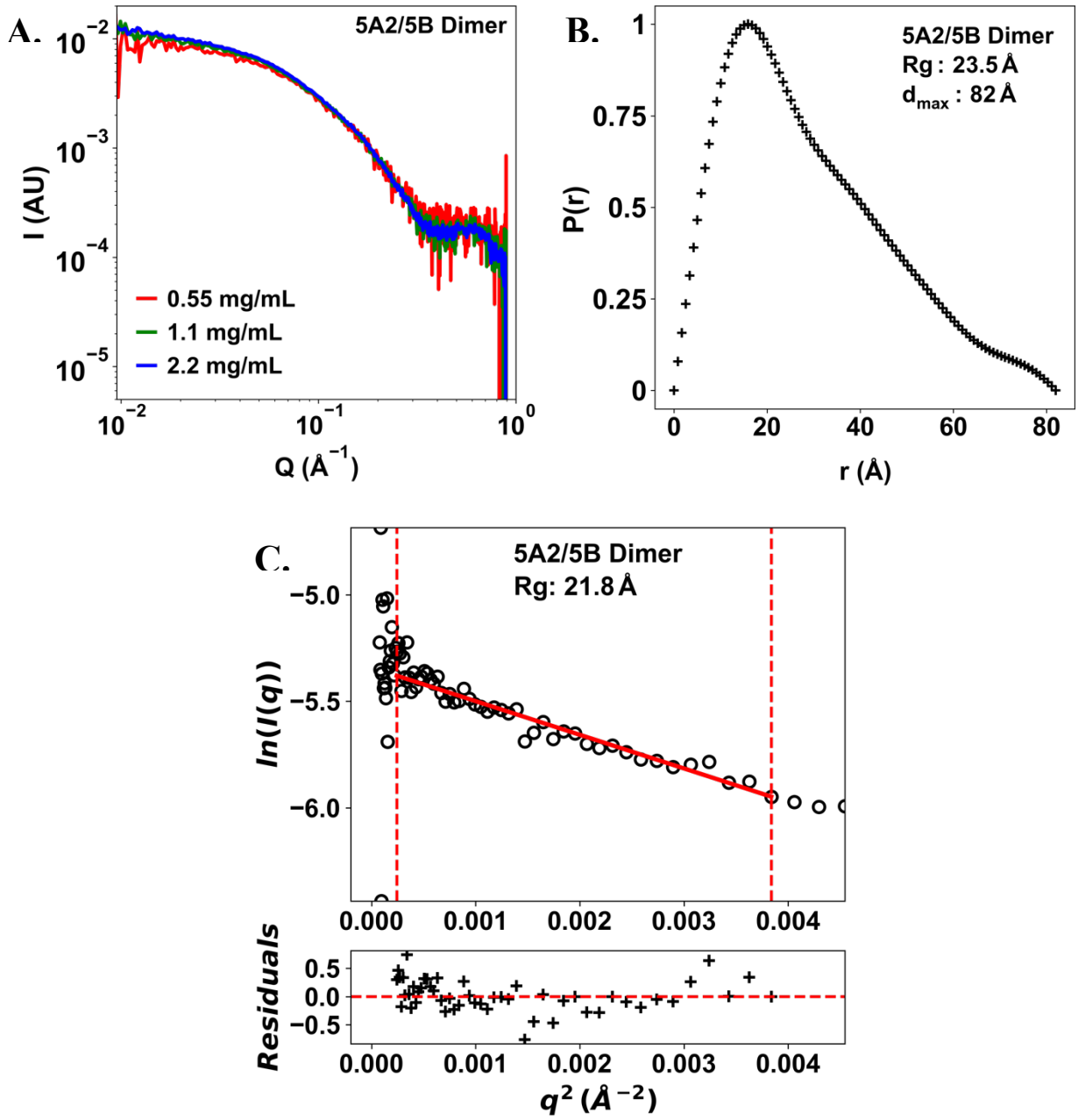

Figure S32. (A) SAXS profiles of the **5A2/5B** dimer at various concentrations. (B) The pair-distance distribution function and (C) the Guinier analysis of the **5A2/5B** dimer using the SAXS data collected at the concentration of 1.1 mg/mL.

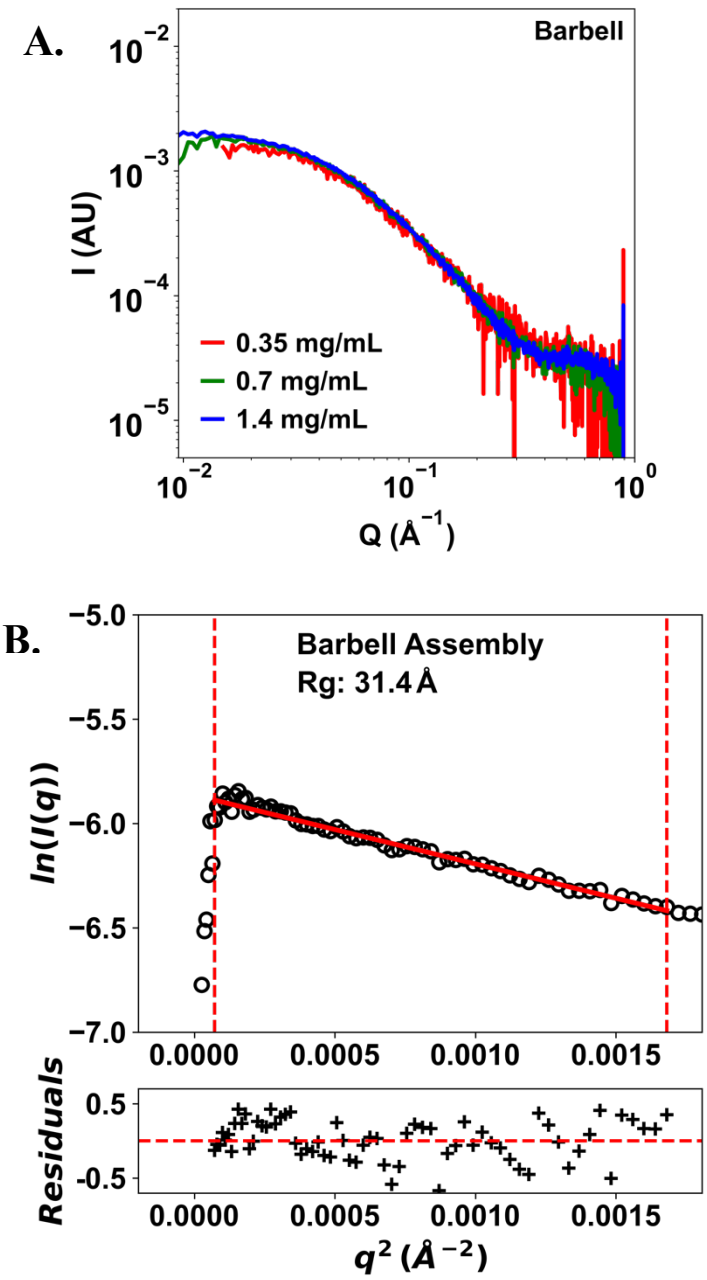

Figure S33. (A) SAXS profiles of the barbell shaped assemblies at various concentrations. (B) Guinier analysis of the barbell shaped assemblies using the SAXS data collected at the concentration of 1.4 mg/mL.

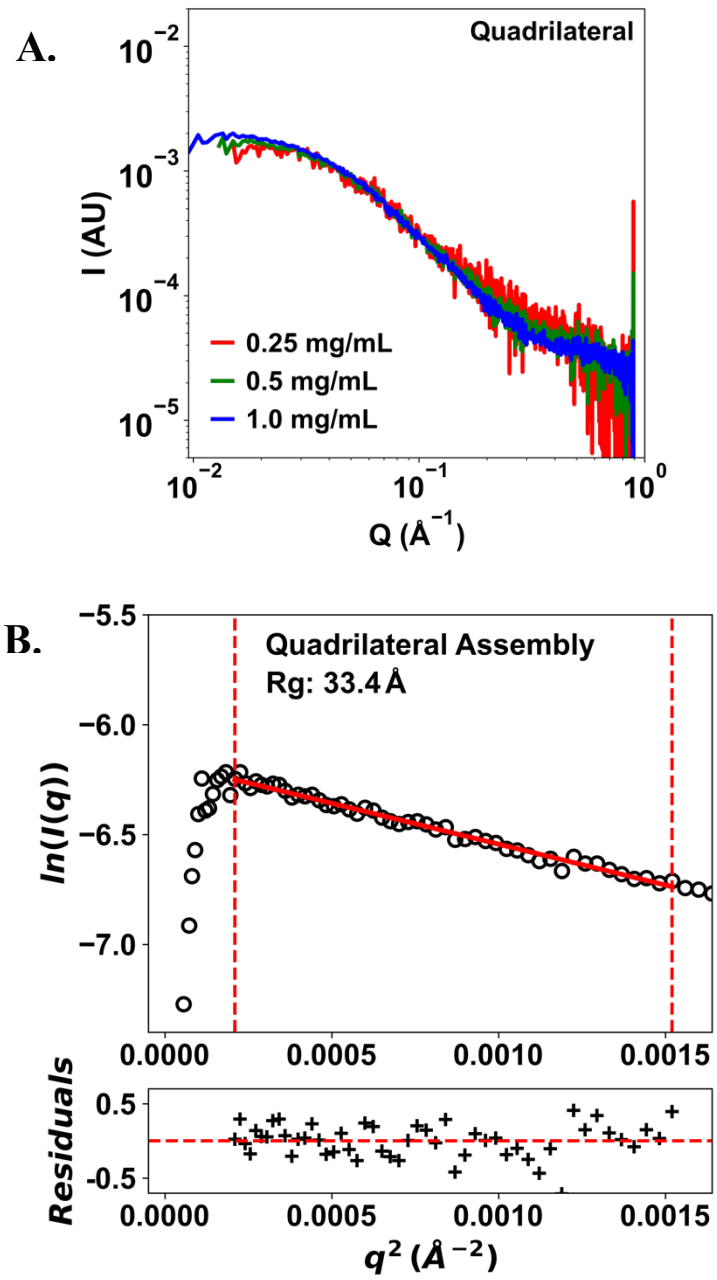

Figure S34. (A) SAXS profiles of the quadrilateral shaped assemblies at various concentrations. (B) Guinier analysis of the quadrilateral shaped assemblies using the SAXS data collected at the concentration of 1.0 mg/mL.

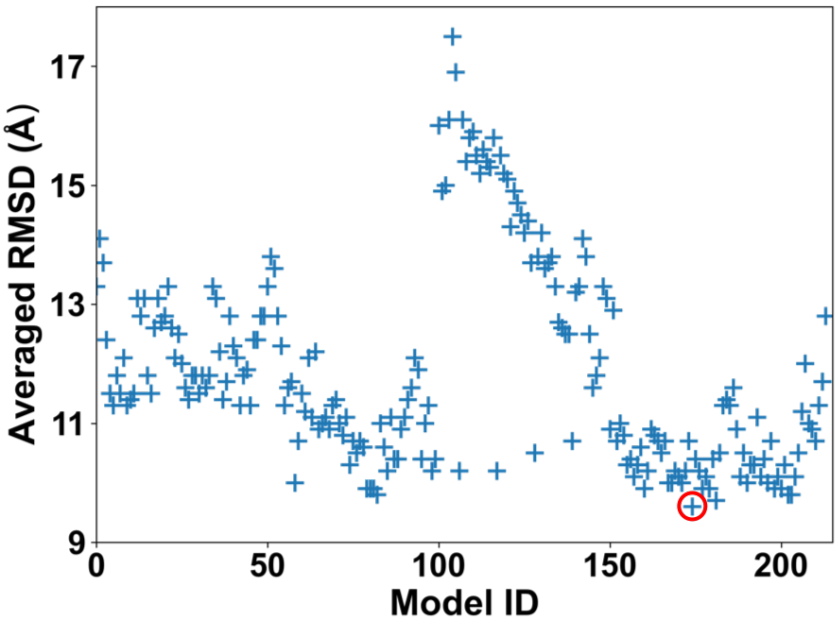

Figure S35. 213 MD models of the barbell shaped assemblies were identified that show good agreement to the experimental SAXS data. Averaged Cα-RMSD values were calculated by using each of these MD models as the reference, as shown in this figure. The model that produced the smallest averaged Cα-RMSD value (highlighted by a red circle) was used as the reference for Cα-RMSD histogram plot in Figure 6A in the main text.

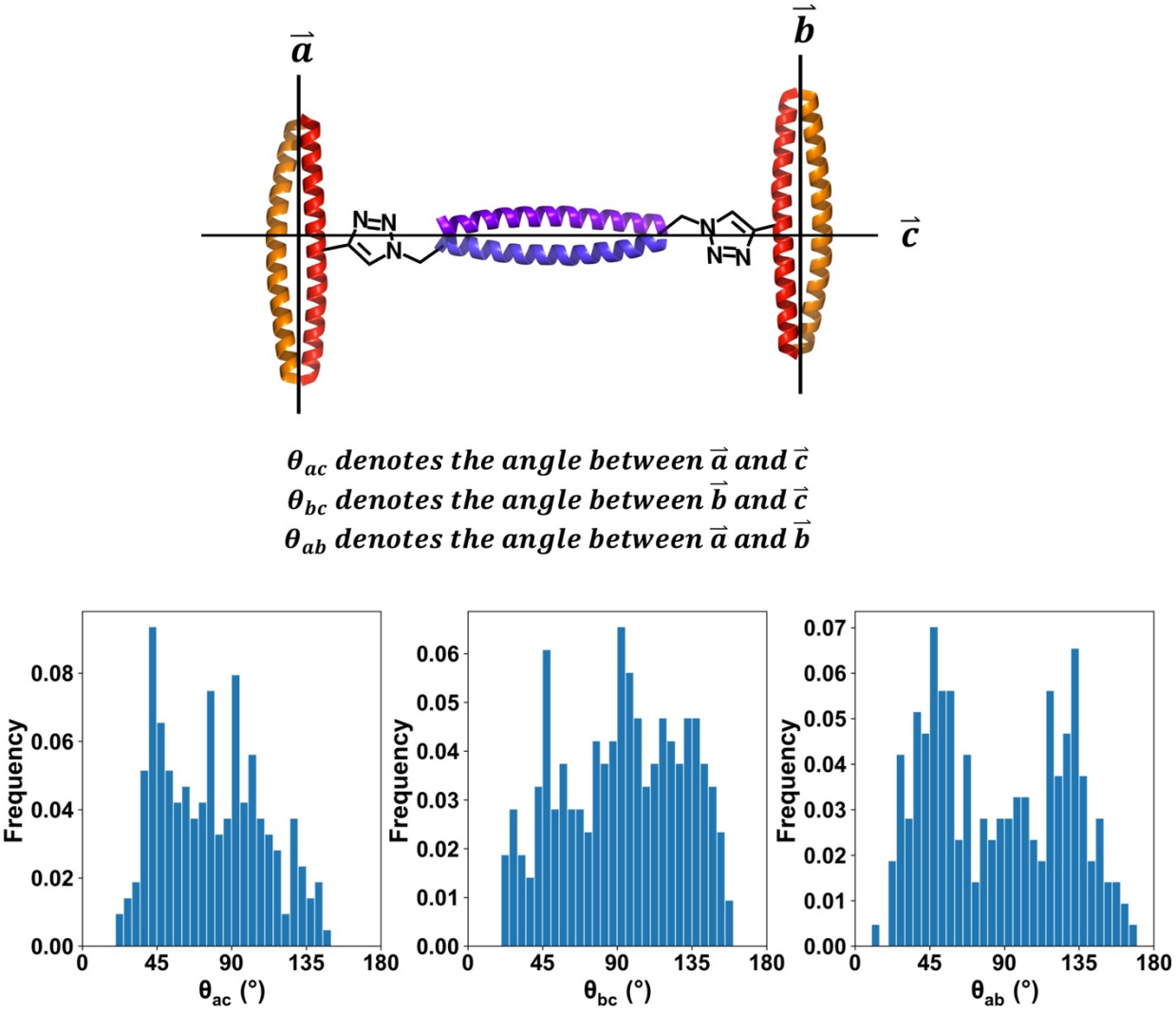

Figure S36. The 213 MD models mentioned in Figure S35 were further analyzed. The angles between the symmetry axes of different dimeric coiled coil components within the barbell shaped assemblies were calculated and plotted as defined above. The broad distrutions of θ_{ac}, θ_{bc} and θ_{ab} reflect the flexibility of the barbell shaped assemblies.

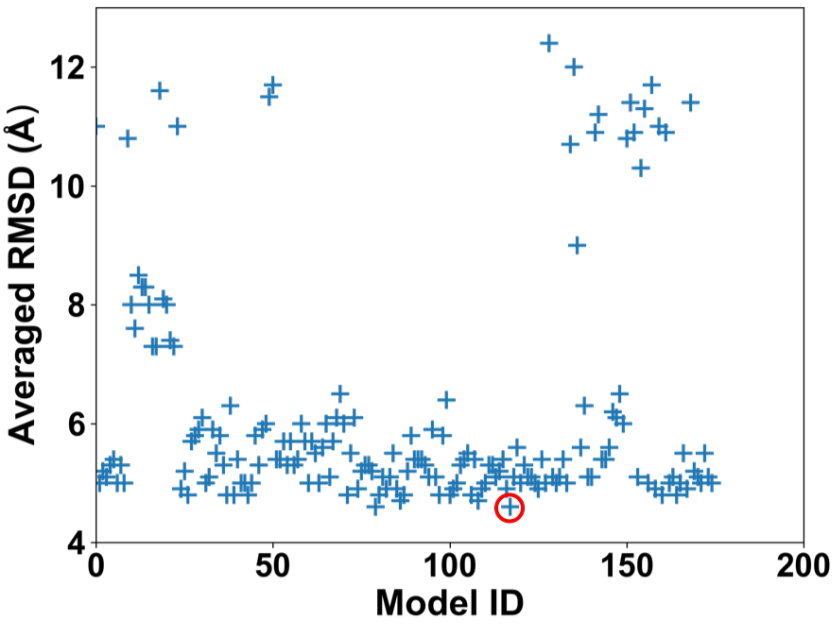

Figure S37. 174 MD models of the quadrilateral shaped assemblies were identified that show good agreement to the experimental SAXS data. Averaged Cα-RMSD values were calculated by using each of these MD models as the reference, as shown in this figure. The model that produced the smallest averaged Cα-RMSD value (highlighted by a red circle) was used as the reference for Cα-RMSD histogram plot in Figure 6B in the main text.

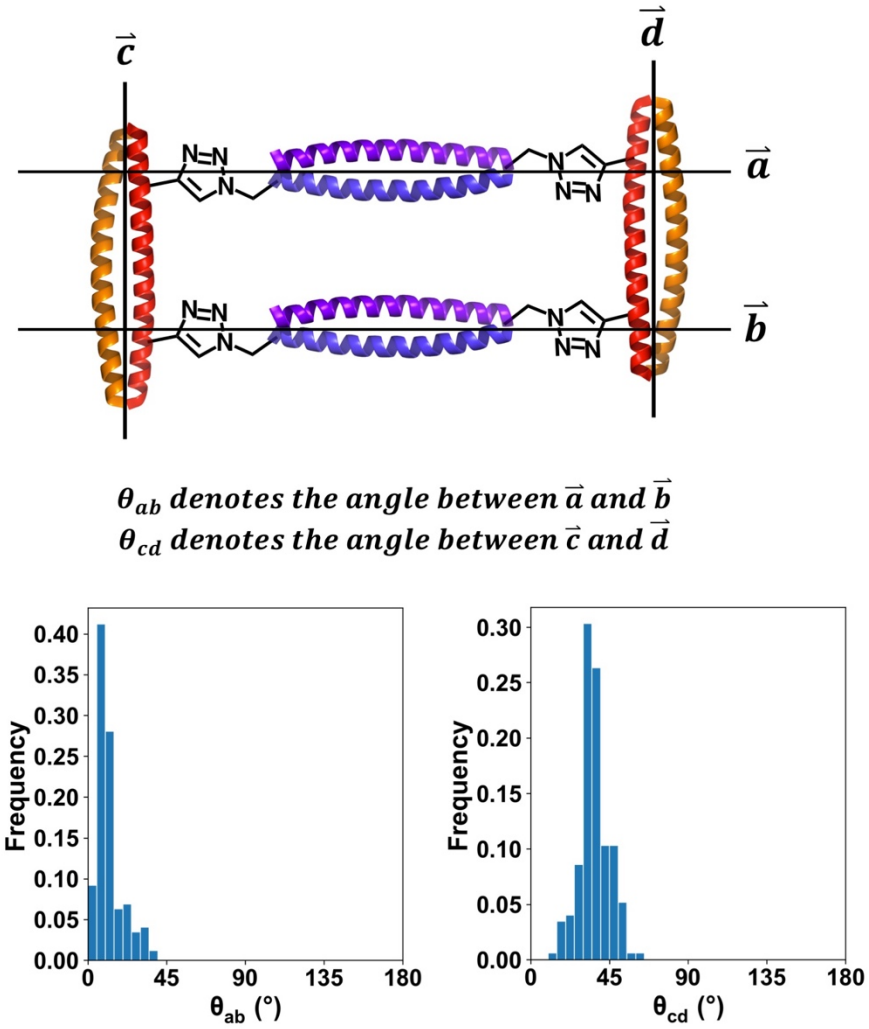

Figure S38. The 174 MD models mentioned in Figure S37 were further analyzed. The angles between the symmetry axes of the two 4A/4B dimeric coiled coils and that of the two 5A2/5B dimeric coiled cils within the quadrilaterl shaped assemblies were calculated and plotted as defined above. The narrow distrutions of θ_{ab} and θ_{cd} reflects the rigidities of the quadrilaterl shaped assemblies.

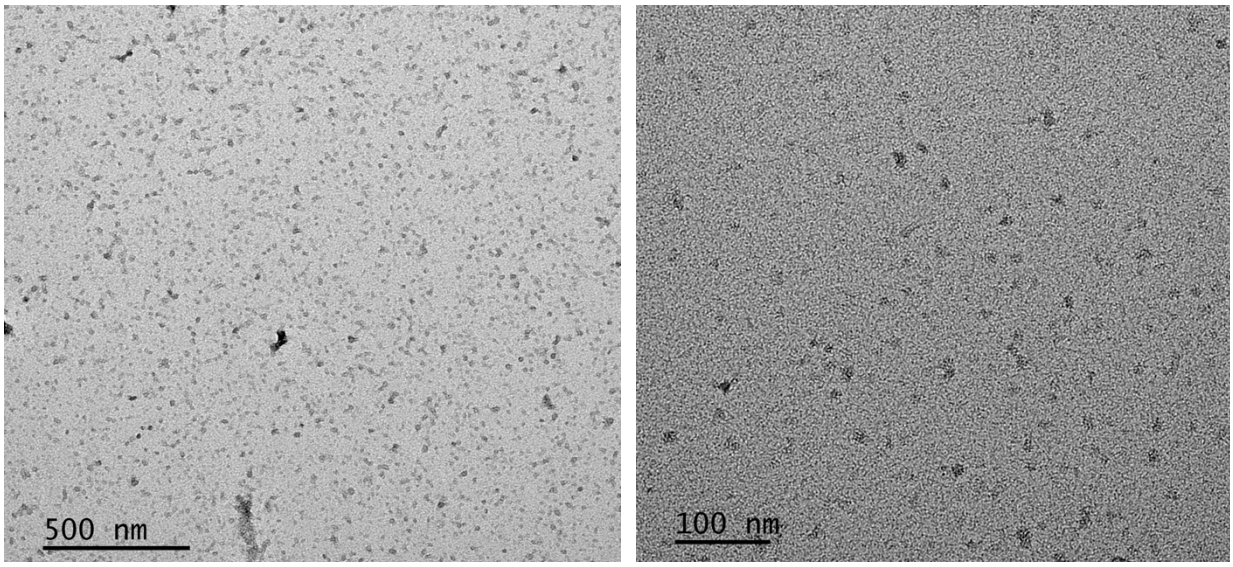

Figure S39. Additional TEM images of the quadrilateral shaped assembly.

References

(1) Michels, T.; Dölling, R.; Haberkorn, U.; Mier, W., Acid-Mediated Prevention of Aspartimide Formation in Solid Phase Peptide Synthesis, *Org. Lett.* **2012,** *14*, 5218-5221.

(2) Jiang, L.; Kirshenbaum, K., A modular approach for organizing dimeric coiled coils on peptoid oligomer scaffolds, *Org. Biomol. Chem.* **2020,** *18*, 2312-2320.

(3) Hopkins, J. B.; Gillilan, R. E.; Skou, S., BioXTAS RAW: improvements to a free open-source program for small-angle X-ray scattering data reduction and analysis, *J. Appl. Crystallogr.* **2017,** *50*, 1545-1553.

(4) Reinke, A. W.; Grant, R. A.; Keating, A. E., A Synthetic Coiled-Coil Interactome Provides Heterospecific Modules for Molecular Engineering, *J. Am. Chem. Soc.* **2010,** *132*, 6025-6031.

(5) Case, D. A.; Belfon, K.; Ben-Shalom, I. Y.; Brozell, S. R.; Cerutti, D. S.; III, T. E. C.; Cruzeiro, V. W. D.; Darden, T. A.; Duke, R. E.; Giambasu, G.; Gilson, M. K.; Gohlke, H.; Goetz, A. W.; Harris, R.; Izadi, S.; mailov, S. A. I.-.; Kasavajhala, K.; Kovalenko, A.; Krasny, R.; Kurtzman, T.; Lee, T. S.; LeGrand, S.; Li, P.; Lin, C.; Liu, J.; Luchko, T.; Luo, R.; Man, V.; Merz, K. M.; Miao, Y.; Mikhailovskii, O.; Monard, G.; Nguyen, H.; Onufriev, A.; Pan, F.; Pantano, S.; Qi, R.; Roe, D. R.; Roitberg, A.; Sagui, C.; Schott-Verdugo, S.; Shen, J.; Simmerling, C. L.; Skrynnikov, N. R.; Smith, J.; Swails, J.; Walker, R. C.; Wang, J.; Wilson, L.; Wolf, R. M.; Wu, X.; Xiong, Y.; Xue, Y.; York, D. M.; Kollman, P. A., AMBER 2020, **2020**, University of California, San Francisco.

(6) Tian, C.; Kasavajhala, K.; Belfon, K. A. A.; Raguette, L.; Huang, H.; Migues, A. N.; Bickel, J.; Wang, Y.; Pincay, J.; Wu, Q.; Simmerling, C., ff19SB: Amino-Acid-Specific Protein Backbone Parameters Trained against Quantum Mechanics Energy Surfaces in Solution, *J. Chem. Theory Comput.* **2020,** *16*, 528-552.

(7) Marion, A.; Gora, J.; Kracker, O.; Frohr, T.; Latajka, R.; Sewald, N.; Antes, I., Amber-Compatible Parametrization Procedure for Peptide-like Compounds: Application to 1,4- and 1,5-Substituted Triazole-Based Peptidomimetics, *J. Chem. Inf. Model.* **2018,** *58*, 90-110.

(8) Izadi, S.; Anandakrishnan, R.; Onufriev, A. V., Building Water Models: A Different Approach, *J. Phys. Chem. Lett.* **2014,** *5*, 3863-3871.

(9) Schneidman-Duhovny, D.; Hammel, M.; Tainer, J. A.; Sali, A., Accurate SAXS profile computation and its assessment by contrast variation experiments, *Biophys. J.* **2013,** *105*, 962-974.

(10) Schneidman-Duhovny, D.; Hammel, M.; Tainer, J. A.; Sali, A., FoXS, FoXSDock and MultiFoXS: Single-state and multi-state structural modeling of proteins and their complexes based on SAXS profiles, *Nucleic Acids Res.* **2016,** *44*, W424-W429.